nature microbiology

ARTICLES

https://doi.org/10.1038/s41564-022-01200-1

Microbial diversity declines in warmed tropical soil and respiration rise exceed predictions as communities adapt

Andrew T. Nottingham[1,2,3]✉, Jarrod J. Scott[3], Kristin Saltonstall[3], Kirk Broders[3,4], Maria Montero-Sanchez[3], Johann Püspök[3], Erland Bååth[5] and Patrick Meir[2,6]

Perturbation of soil microbial communities by rising temperatures could have important consequences for biodiversity and future climate, particularly in tropical forests where high biological diversity coincides with a vast store of soil carbon. We carried out a 2-year in situ soil warming experiment in a tropical forest in Panama and found large changes in the soil microbial community and its growth sensitivity, which did not fully explain observed large increases in CO_2 emission. Microbial diversity, especially of bacteria, declined markedly with 3 to 8 °C warming, demonstrating a breakdown in the positive temperature-diversity relationship observed elsewhere. The microbial community composition shifted with warming, with many taxa no longer detected and others enriched, including thermophilic taxa. This community shift resulted in community adaptation of growth to warmer temperatures, which we used to predict changes in soil CO_2 emissions. However, the in situ CO_2 emissions exceeded our model predictions threefold, potentially driven by abiotic acceleration of enzymatic activity. Our results suggest that warming of tropical forests will have rapid, detrimental consequences both for soil microbial biodiversity and future climate.

Microbial communities sustain the biosphere by cycling carbon (C) and nutrients between the Earth and the atmosphere. As a result, their response to warming provides fundamental feedback on the terrestrial C cycle and climate, and will have direct consequences for the function and maintenance of terrestrial biota[1]. The nature of this feedback is especially critical for tropical forests because they exchange more carbon dioxide (CO_2) with the atmosphere than any other ecosystem, contain over a third of global soil C[2] and two-thirds of terrestrial plant biomass[3], and represent the apex of global terrestrial biodiversity[4]. Under current emission scenarios, temperatures in the tropics are predicted to warm by 2–5 °C by 2100[5] and to exceed historical precedent more quickly than anywhere else on Earth[6]. Despite this, we have almost no information on the magnitude and direction of soil microbial feedbacks under warming for the huge C stores and biodiversity found in tropical forests[7].

Climate warming is predicted to increase the mineralization of soil organic matter and consequently, the emission of CO_2 from soil to the atmosphere[8]. Numerous experiments performed outside the tropics have shown that warming increases CO_2 emission from soil[9], and that changes in the activity and community composition of soil microbes influence the associated soil C loss[10,11]. In tropical forests where soils contribute a major portion of these ecosystems' globally important total C exchange with the atmosphere[12], small fractional increases in CO_2 emission from soils will have a large impact on the atmosphere and climate. Warming experiments in tropical forests have only recently been initiated[13,14] and first results point towards a large response. Two years of in situ full-profile soil warming by an average 4 °C increased the soil CO_2 efflux by 55% for a tropical forest in Panama[13]. This result provokes key fundamental questions: what are the drivers of the large CO_2 emissions from warmed tropical forest soils and are they related to abiotic or biotic processes, including changes in the composition of the microbial community, its diversity and/or its activity, as found in other ecosystems[10,11,15]?

The response of soil C to warming is underpinned by changes in soil microbial activity via the instantaneous sensitivity of microbial growth and respiration, which can be modified over time by adaptive change in the microbial community composition[10,16]. These microbial responses have been represented in models of soil C temperature sensitivity by the efficiency of growth and respiration[17], while the thermal response of growth and respiration has been described by the square root model[16,18]. In the square root model, the moderating effect of temperature adaptation is described by a change in the theoretical value of T_{min} (the minimum temperature for growth), corroborated by observations that T_{min} is strongly correlated with mean annual temperature differences across climatic gradients globally[19–21]. For example, T_{min} for bacterial growth ranges from approximately −15 °C in Arctic ecosystems to approximately 0 °C for tropical ecosystems, with similar patterns observed for the optimal temperature of growth (T_{opt})[16,20] and for respiration[21]. Across temperate temperature ranges, T_{min} has been observed to increase under experimental warming[22,23] alongside community compositional shifts[15,24,25], thus indicating that the observed thermal adaptation occurred via microbial community composition change. Despite the proven importance of this relationship in determining the temperature response of activity and its thermal adaptation[16,18], we have no information on whether it holds under warming in the lowland tropics, where the mean annual temperature is already close to the predicted optima for metabolic activity[16].

[1]School of Geography, University of Leeds, Leeds, UK. [2]School of Geosciences, University of Edinburgh, Edinburgh, UK. [3]Smithsonian Tropical Research Institute, Balboa, Ancon, Republic of Panama. [4]Mycotoxin Prevention and Applied Microbiology Research Unit, National Center for Agricultural Utilization Research, Agricultural Research Service USDA, Peoria, IL, USA. [5]Section of Microbial Ecology, Department of Biology, Lund University, Lund, Sweden. [6]Research School of Biology, Australian National University, Canberra, Australia. ✉e-mail: A.Nottingham@leeds.ac.uk

The effect of warming on tropical forest soil C will depend not only on the response of the soil microbial community activity[7], but also its community composition and diversity, which may have consequences for other biota[26]. In a temperate forest, two decades of experimental warming increased bacterial diversity[15], specifically for lignin-degrading microbes;[27] this positive temperature-diversity relationship is consistent with observations across natural temperature gradients where soil pH and moisture are held constant[24,28,29], although exceptions to this pattern may occur[30]. It is unknown whether soil microbial diversity will similarly increase under the novel high-temperature regimes predicted for the tropics[6] and will depend on the thermal tolerance of the microbial taxa present[25,31]. Nor is it understood how diversity change would affect soil process rates, although the effect might be considerable, given phylogenetic evidence for high niche specialization among tropical forest microbial taxa[32]. The historically novel high-temperature regimes predicted for the tropics this century[6] (for example, 2–5 °C atmospheric warming[5] added to 1–3 °C warming through land-use change and reduced transpiration[33]) could result in temperature maxima that exceed a metabolic threshold for portions of the tropical forest soil microbial community, with potentially large implications for ecosystem functioning and the climate.

Here we used an in situ warming experiment to test the response of the soil microbial community, and its growth and respiration to warming over a range of 3 to 8 °C above ambient, thereby providing a test of how tropical forest soil communities and function respond across these levels of warming in a field experiment. The experiment, SWELTR (Soil Warming Experiment in Lowland TRopical forest), consists of five pairs of circular control and warmed plots (whole-profile warming, using buried resistance cables) distributed evenly within approximately 1 ha of semi-deciduous moist lowland tropical forest on Barro Colorado Island, Panama[13]. Each warmed plot has a ground surface area of ~20 m^2 and is heated across the full soil profile, resulting in a total of 120 m^3 of warmed soil for the experiment (Extended Data Fig. 1). For this study, we established two subplots per treatment plot that differed with distance to the heating source, thus providing two treatments of, on average, 3 °C and 8 °C warming of surface soils (0–20 cm depth). Two years after the warming treatment was initiated, we conducted field campaigns during the wet season (when moisture was non-limiting) to measure soil CO_2 efflux, to characterize the temperature sensitivity of instantaneous microbial growth, respiration and enzyme activities, and to determine the microbial community composition. We tested the hypotheses that: (1) warming will change the α-diversity and community composition of soil bacteria and fungi; (2) the temperature sensitivity of microbial communities (with respect to growth, T_{min} and enzymatic activity) will become 'adapted' to the new temperature regime (whether adaptation is via genetic change within species, phenotypic plasticity or community-composition change, sensu Pietikäinen et al.[34] and Bradford[35]); and (3) soil CO_2 emission will increase under 3 to 8 °C warming and follow the increase predicted by the temperature sensitivity of microbial growth and respiration.

Results

Microbial diversity. Two years of soil warming reduced the diversity of both bacteria and fungi, and caused large shifts in the microbial community composition (Fig. 1, Extended Data Tables 1 and 2). The diversity decline was largest for bacteria, occurring via the loss of proportionally abundant taxa (Shannon and Inverse-Simpson indices declined; Fig. 1 and Extended Data Fig. 2). For fungi, our results suggest a diversity decline due to loss of rare taxa (species richness declined but not Shannon and Inverse-Simpson indices), although this result is less definitive than that for bacteria, given methodological issues influencing the detection of rare taxa (see Supplementary Methods) and our identification of different fungal taxa in warmed soils (see below). Warmed soils also hosted microbial species (defined by amplicon sequence variants, ASVs) that were undetected in soils at ambient temperature, especially among fungi, although the number of newly detected species was too few to offset the number of species no longer detected (Fig. 1). This decline in diversity, especially for the bacteria, may have implications for soil functioning, given the prevailing paradigm of a positive relationship between biological diversity and ecosystem functioning[36], also supported for soils[37,38]. Such a decline in soil microbial diversity under warming is also contrary to positive relationships between temperature and diversity observed in a temperate forest warming experiment[15] and across natural environmental gradients[28,29,39]. This positive relationship is consistent with the metabolic theory of ecology (that is, a positive correlation between energy input, evolutionary rates and diversity)[40] and is considered to be one of several positive feedbacks on tropical plant diversity[41–43]. Our results point towards a breakdown in this energy-diversity relationship for tropical soil bacterial communities after a 2-year period where temperatures ranged from 29–34 °C. These temperatures may represent a thermal maximum for the persistence of many species, implying that our findings can also provide insight over timescales longer than the duration of our warming treatment.

Microbial community composition. Warming also caused large shifts in community composition (Figs. 1 and 2, and Extended Data Figs. 2–5), with many taxa significantly increasing or decreasing in relative abundance with warming by 3 °C, and further with warming by 8 °C (Fig. 1, and Extended Data Figs. 3 and 4). In warmed soils, there was a decrease in the relative abundance of Bacteroidetes, a common non-spore-forming bacterial group which comprise taxa that are primary degraders of polysaccharides[44]. For fungi, there was decrease in the relative abundance of members of the Basidiomycota including the Agaricales, a broad order of saprophytic and ectomycorrhizal fungi, and the ecologically diverse yeast order, Sporidiobolales. In contrast, warming increased the relative abundance of Firmicutes, a diverse and stress-tolerant bacterial phylum able to form endospores resistant to desiccation and high temperatures[45]. Indeed, taxa within the Firmicutes have been identified as warm-responsive in laboratory studies[25,31] and in field soil warming experiments outside the tropics[15,30,46]. Warming also increased the abundance of the class Thermoleophilia within the Actinobacteria, known to include aerobic thermophiles[47]. For fungi, warming increased the relative abundance of Glomerales—arbuscular mycorrhizae—as also seen in warming experiments outside the tropics[48]. In addition, warming increased the relative abundance of several orders in the phylum Ascomycota, including the Eurotiales, Hypocreales and Pezizales, which include thermotolerant saprophytic and pathogenic species, as well as saprophytic and pathogenic yeast in the Saccharomycetales. Thus broadly, changes in diversity under warming occurred alongside shifts in communities towards thermotolerant microorganisms.

Growth adaptation to temperature. Adaptation of the microbial community to warming can potentially have a large influence on long-term change in soil C emissions[10,17]. To assess this, we used laboratory incubations to determine the instantaneous temperature sensitivity of bacterial growth (T_{min}) following the square root model[16,18], whereby changes in T_{min} reflect a community adaptation to temperature, a response empirically related to shifts in the community composition[25]. In the square root model, the effect of temperature on activity is described by a quadratic increase up to T_{opt}, and then a sharp decline[16,18] where the quadratic phase of the increase is constrained by the T_{min} (the y-intercept of the square root of activity plotted against temperature), which is higher for microbial communities adapted to warmer temperatures[16]. Following 2 years of experimental warming at our tropical forest site, we found T_{min} to increase under 3 °C warming

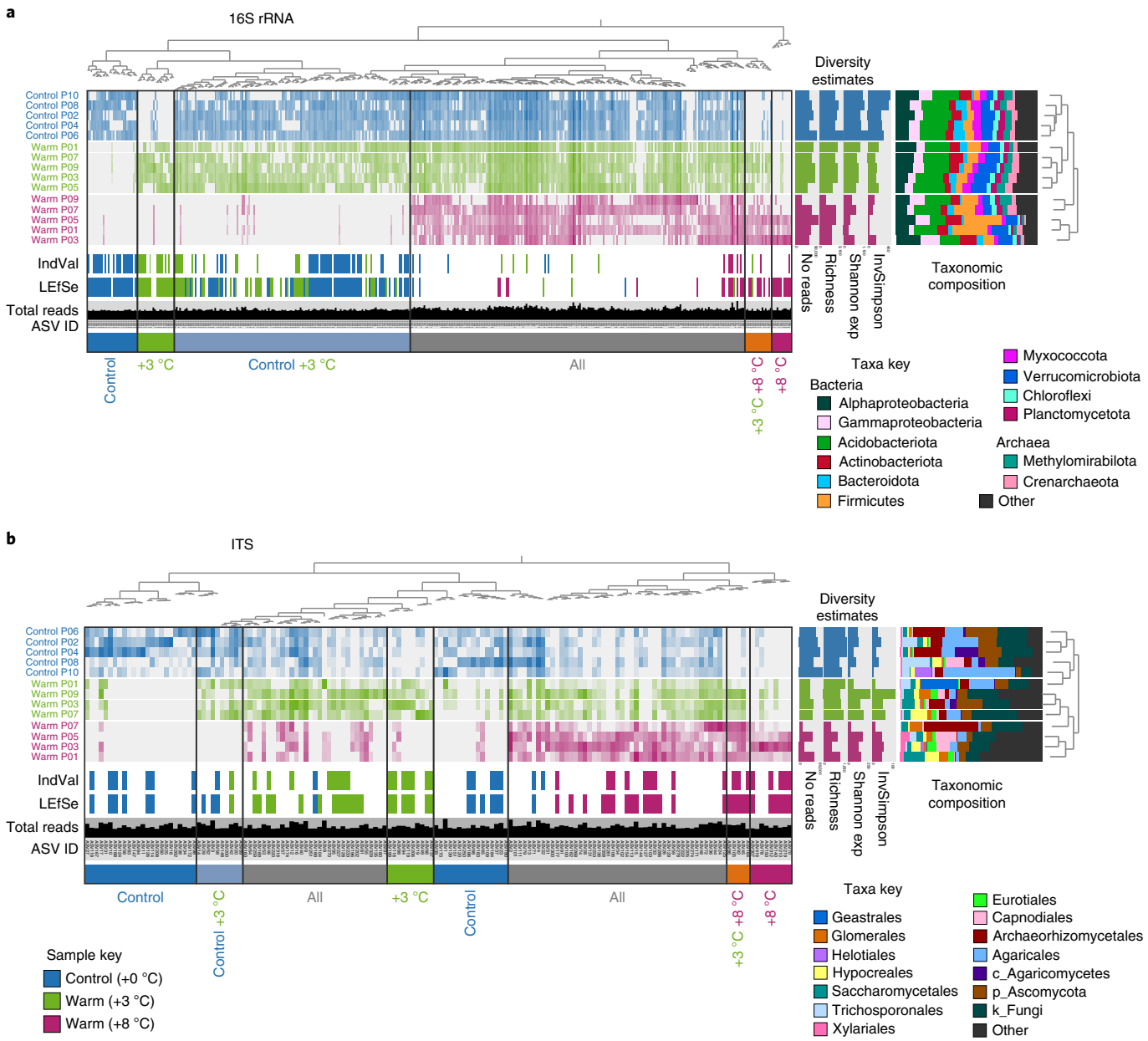

Fig. 1 | Microbial diversity decline and community change under in situ soil warming in lowland tropical forest. a,**b**, Two years of soil warming (3 ºC and 8 ºC) caused significant decreases in bacterial (**a**) and fungal (**b**) diversity, determined by 16S rRNA and ITS sequencing, respectively. Data from the PIME-filtered datasets for controls (blue), 3 °C warming (green) and 8 °C warming (red). Hierarchical clustering of ASVs (left dendrograms) is based on Euclidean distance and Ward linkage. Hierarchical clustering of samples (right dendrograms) is based on Bray-Curtis distance and complete linkage. Each vertical line in the main plot represents a unique ASV, where colour intensity indicates the log-normalized abundance, and no colour indicates an ASV that was either not detected or was removed during prevalence filtering. The coloured bars below indicate ASVs that were enriched in different temperature treatments as determined by either indicator species analysis (IndVal) or linear discriminant analysis effect size (LEfSe). Additional data for each sample are presented in the plots on the right. Diversity estimates charts show the total number of reads, observed richness, Shannon exponential index and Inverse-Simpson index. Taxonomic profiles show the proportion of major classes (16S rRNA data) or orders (ITS data). All analyses are for soil samples collected from $n = 5$ independent experimental plots for each treatment level.

and to increase further under 8 °C warming (Fig. 2); where the observed magnitude of increase in T_{min} of 0.3 °C per 1 °C warming is consistent with observations made elsewhere[16]. Furthermore, among all the parameters associated with temperature adaptation in the field experiment, T_{min} was the most significant correlate of the change in bacterial and fungal diversity and community composition (Fig. 2e, and Extended Data Tables 1 and 2). Thus, while acknowledging that we cannot exclude an influence of genetic change within species on this temperature adaptation, our results strongly suggest that adaptation occurred through community compositional change, as found elsewhere[25], and the development of a microbial community functionally adapted to the warmer conditions.

Soil process rates. The changes in diversity and community composition occurred alongside altered soil process rates in the field experiment: increased bacterial growth rates, enzyme activity per

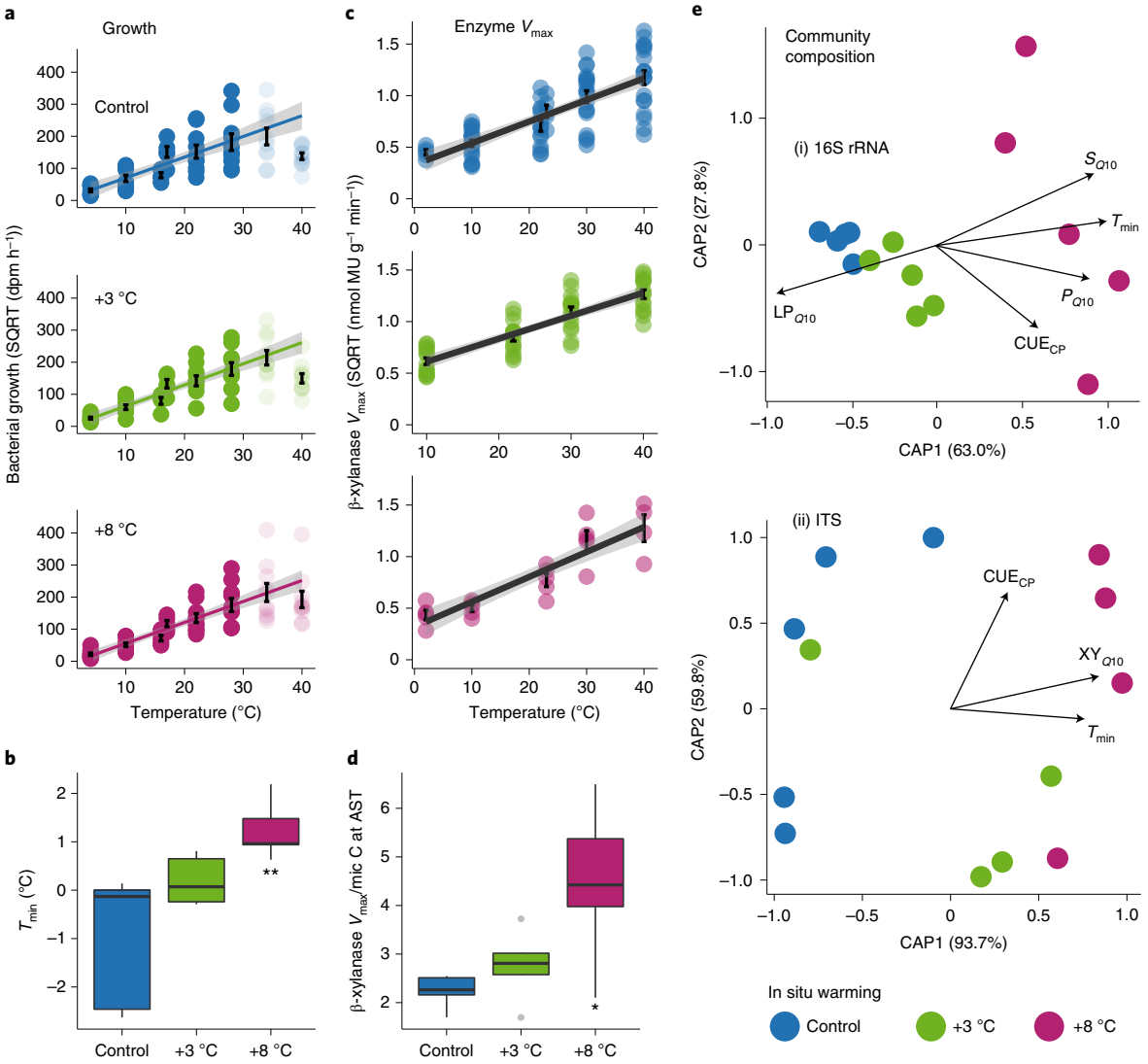

Fig. 2 | Response of microbial growth and enzyme activity to soil warming, and the relationship between this temperature response and microbial community changes. a, Microbial growth was determined for bacteria for each treatment (control, +3 °C and +8 °C) using Leu-incorporation incubation assays across a temperature range of 4–40 °C. **b**, T_{min} increased with warming ($P = 0.006$ for +8 °C treatment), but growth declined at high temperatures (>30–34 °C; lighter shaded points in **a**; these data were not used for the linear model to determine T_{min}). **c**, Activities were determined for 10 enzymes (ß-xylanase shown here, six others responded similarly; see Supplementary Information) across an incubation temperature range of 4–40 °C. **d**, The maximum potential activity (at soil temperature, AST, per unit microbial C) increased with warming for 7 out of 10 enzymes (ß-xylanase shown here) and increased across high temperature ranges (to 40 °C), illustrating a decoupling of growth and activity above 30 °C. **e**, The microbial community composition change was related to the temperature response of growth (T_{min}) and of enzyme activities (Q_{10} of V_{max}) for bacteria (**i**) and fungi (**ii**). Bacterial growth and enzyme activity are plotted using a linear transformation (square root). Microbial community composition change estimated using db-RDA based on Bray-Curtis dissimilarity; see Extended Data Tables 1 and 2 and Fig. 5 for relationships between richness or community composition change and other soil properties. For scatterplots (**a** and **c**), the error bars represent mean ± 1 s.e.m. for $n = 5$ plots. Fitted lines depict linear functions with 95% confidence intervals. For boxplots (**b** and **d**), the centre line represents the median, the lower and upper bounds represent the first and third quartiles, and whiskers represent +1.5 the interquartile range. *$P = 0.016$ in **d**, **$P = 0.006$ in **b** (by ANOVA). All analyses are for soil samples collected from $n = 5$ independent experimental plots for each treatment level.

unit microbial biomass for 7 hydrolytic and oxidative enzymes involved in C, nitrogen (N) and phosphorus (P) cycling (although microbial biomass remained stable) and increased soil CO_2 emission, measured in situ (Figs. 2 and 3, and Extended Data Figs. 6 and 7). Soil CO_2 emission in the field experiment increased markedly at warmer temperatures: 78% higher than controls under 3 °C warming and 337% higher under 8 °C warming of surface soils (Fig. 3 and Extended Data Table 3). The soil CO_2 efflux response for the wet season was consistent with the previously reported 55% increase over 2 years of 3 °C surface soil warming at this experiment (including dry and wet seasons), which was shown to have arisen predominantly from increased heterotrophic microbial activity[13]. Our observation of increased soil metabolic activity, indicated by increased bacterial growth and enzyme activity with in situ soil warming, describes a further acceleration of heterotrophic activity with warming. Enzymatic activity per unit of microbial biomass increased for 7 out of 10 studied enzymes and markedly at +8 °C in situ warming for enzymes that degrade organic phosphorus, nitrogen and carbon in phenolic and hemicellulose compounds (Fig. 2, and Extended Data Figs. 6 and 7). Collectively, the observed

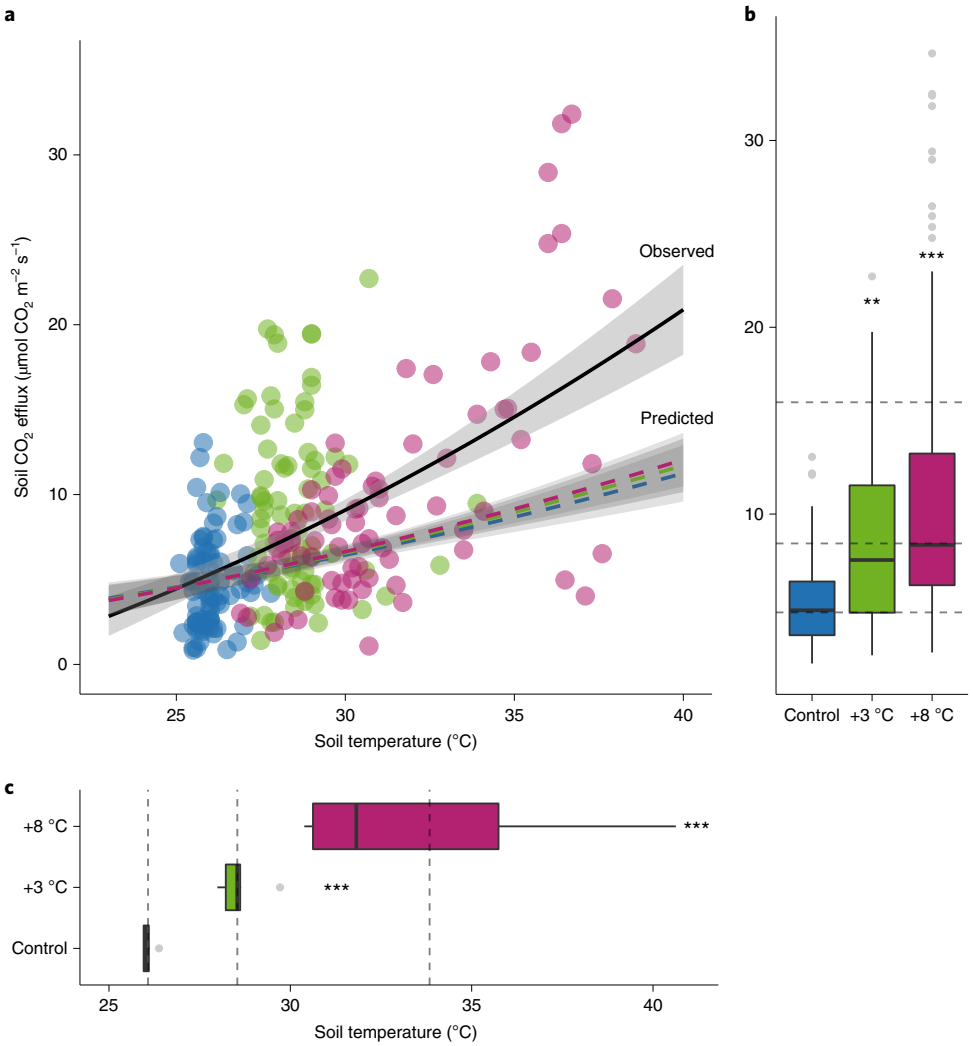

Fig. 3 | The response of soil CO_2 efflux to in situ warming is greater than the increase predicted by the temperature response of microbial respiration and growth. a, Data points are measurements of soil CO_2 efflux from control (blue), 3 °C warming (green) and 8 °C warming (red). The response of CO_2 emission to temperature was described by a square root function ('Observed' line; $CO_2 = 1.9 \times T^2 - 45$; $R^2 = 0.68$, $P < 0.001$, $F = 556$). The modelled CO_2 efflux responses ('Predicted' lines) are based on measured T_{min} at ambient temperature (blue dashed line, no adaptation; $CO_2 = 1.21 \times T^2 - 0.17$; $R^2 = 0.87$, $P < 0.001$, $F = 124$) and T_{min} change after 2 years of warming indicating community adaptation (green dashed line, 3 °C adaptation; $CO_2 = 1.24 \times T^2 - 0.18$; $R^2 = 0.87$, $P < 0.001$, $F = 118$; and red dashed line, 8 °C adaptation; $CO_2 = 1.25 \times T^2 - 0.20$; $R^2 = 0.86$, $P < 0.001$, $F = 111$). Lines depict square root functions with 95% confidence intervals (grey shading). **b**,**c**, Boxplots show the treatment effects on soil CO_2 efflux (**b**) and soil temperature (**c**) (repeated measures ANOVA; $^{**}P < 0.01$; $^{***}P < 0.001$; treatment effects on soil CO_2 efflux were $P = 0.00392$ and $P < 0.001$ for 3 °C and 8 °C warming, respectively). The soil temperature and soil CO_2 efflux by treatment are: for controls: 26 ± 1 °C and 4.74 ± 0.25 μmol CO_2 m^{-2} s^{-1}; 3 °C warming: 29 ± 2 °C and 8.42 ± 0.44 μmol CO_2 m^{-2} s^{-1}; 8 °C warming: 34 ± 7 °C and 15.98 ± 1.68 μmol CO_2 m^{-2} s^{-1} (mean ± 1 s.e.m., $n = 5$ plots). The centre line of each boxplot represents the median, the lower and upper bounds represent the first and third quartiles, and whiskers represent +1.5 the interquartile range; the dashed lines represent means. All analyses are for soil samples collected from $n = 5$ independent experimental plots for each treatment level.

changes in process rates—increased respiration, growth and enzymatic activity per unit microbial biomass—corroborate our parallel findings that the microbial community shifted towards favouring thermotolerant taxa that readily persist and even increase in productivity under warmer conditions.

Predicted and observed soil CO_2 emission under warming. We used the instantaneous temperature sensitivity of bacterial growth (T_{min}) to model the CO_2 efflux response to warming, both with (T_{min} determined for soil from warmed treatments) and without (T_{min} determined for soil from controls) microbial community temperature adaptation. Here we used T_{min} only for bacterial growth because there was no significant difference in the T_{min} for bacterial growth (−1.4 ± 0.8) and respiration (0.3 ± 0.4) in control soils ($P = 0.1$). The T_{min} values for bacterial growth in control soils were also similar to those determined independently for two lowland tropical forests in Peru with similar mean annual temperature (−1.66 ± 0.7, −1.77 ± 1.0; MAT = 26.4 °C)[20]. To model the CO_2 efflux response to warming following temperature adaptation of microbial communities, we refitted the Ratkowsky model (see methods) using the T_{min} determined for bacterial growth in experimentally warmed soils for 2 years by 3 °C and 8 °C ('adapted' communities).

The predicted increase in soil CO_2 efflux based on the measured temperature sensitivity of microbial respiration and growth in control soils (24–68% increase under 3–8 °C warming; Fig. 3) was substantially exceeded by the observed in situ increase in soil CO_2 efflux (78–337% under 3–8 °C warming; Fig. 3). Furthermore, the predicted CO_2 emission was only marginally higher when accounting

for adaptation of the microbial community to warmer conditions (measured T_{min} increase; Fig. 2), resulting in a 25–77% increase under 3–8 °C warming (Fig. 3). Importantly, we found no evidence to suggest that the observed in situ increase in soil CO_2 emission occurred due to decreased microbial metabolic efficiency, a common finding in short-term soil warming experiments where high waste respiration exceeds growth[49]. Reduced metabolic efficiency is inconsistent with our previously reported observation of no decrease in the size of the microbial biomass or in microbial carbon-use efficiency[50] (measured using a stoichiometric method, see Methods for discussion of this method and its assumptions; Extended Data Fig. 6), a result in line with the independent observation of increased microbial biomass under soil warming in a tropical forest in Puerto Rico[51]. Similarly, we cannot explain the augmented soil CO_2 emission by reference to accelerated substrate depletion or substrate depletion alongside priming effects where microbes acquire additional N or P from organic sources[52], which would also be expected to cause an eventual decline in microbial biomass[50,53]. On the contrary, we found no change in microbial biomass despite evidence for substrate depletion (decreased dissolved organic C and available P at 8 °C warming; Extended Data Fig. 6).

Soil warming can also induce soil drying, potentially influencing CO_2 emission and other community and process rate changes[8]. However, our study here was focused on the tropical rainy season and despite lower moisture content in our +8 °C treatment (Extended Data Fig. 6), we expect that this had negligible influence on our results because moisture remained non-limiting to microbial activity. Finally, the augmented in situ soil CO_2 emission cannot be explained by increased root respiration or substrate supply from root exudates because, by using root-partitioning cores, we found that warming had no effect on the root-derived soil CO_2 efflux[13]. Thus, we show that the temperature response of microbial community metabolism to warming—considered in models to be fundamental in explaining the long-term and relatively large response of soil C to climate warming[17,50]—only accounted for 23–32% of the observed in situ soil CO_2 emission.

Abiotic processes may increase CO_2 emissions. In addition to biotic processes, our data point towards a further influence of abiotic processes in accelerating CO_2 emission at warmer temperatures. By using ex situ soil incubations across 2–40 °C, we found that microbial growth declined at temperatures exceeding 34 °C (Fig. 2); however, enzyme activities measured under both ex situ and in situ warming increased, as did in situ soil CO_2 emissions (Figs. 2 and 3, and Extended Data Figs. 6 and 7). These results can be explained by the effect of warming on the soil physico-chemical environment, including chemical oxidation/hydrolysis and desorption of mineral-stabilized organic matter and extracellular enzymes[54]. Clay-rich soils, such as those found at our tropical forest site, contain a large pool of stabilized C and inactive extracellular enzymes adsorbed to clay minerals[55]. At high temperatures, desorption reaction rates can overtake adsorption reaction rates[56], thereby increasing the pools of active enzymes and labile C, and consequent CO_2 emissions. Independent observations support this mechanism of an abiotic contribution to enzyme activity under warming: high respiration and enzymatic activity in sterilized soils[57,58], and stable enzyme functioning at high temperatures[59]. Consistent with a rapid increase in the pool of active enzymes driven by desorption, under warming we observed increased Q_{10} of V_{max} for four enzymes including phosphomonoesterase, β-xylanase and β-glucosidase (Fig. 2 and Extended Data Fig. 6). This is counter to the prediction of reduced Q_{10} for 'warm-adapted' iso-enzymes thought to result from increased folding and decreased flexibility[56,60] but is consistent with a rapid increase in the pool of active enzymes under warming, driven by desorption reactions[61].

Enhanced soil CO_2 emissions driven by accelerated enzyme activities under warming could also occur through chemical oxidation. Under aerobic conditions, oxides of Fe and Mg minerals—abundant in many tropical soils including at our study site—provide electron acceptors that catalyse the degradation of phenol compounds and the formation of reactive organic compounds[58,62]. Because we focused on responses during the wet season when moisture was non-limiting, soil drying at higher levels of warming might have increased O_2 supply, increasing the activity of oxidative enzymes and organic matter oxidation[58,62,63]. Consistent with this mechanism, soil moisture declined at 8 °C (although not to the extent to cause moisture limitation; Extended Data Fig. 6) alongside a marked increase in the activity of phenol oxidase (Extended Data Table 3). It is therefore possible that a combination of these processes resulted in increased enzyme activity that was uncoupled from growth (Fig. 2), contributing substantially to the observed CO_2 emissions that exceeded the predicted increase based on standard expectations from the observed temperature sensitivity and warm-adaptation response of the microbial community[16] (that is, it was exceeded by 3.1–4.4 fold; Fig. 3).

Discussion

In summary, our results show a progressive decline in tropical forest soil microbial diversity, especially for bacteria, and marked microbial community compositional shifts with warming (Fig. 1), occurring alongside community growth-adaptation to temperature (Fig. 2) and resulting in further increased CO_2 emission (Fig. 3). This response of diversity declines under warming is contrary to observations from temperate forest warming studies[15,27]. Our data thus provide empirical support for the hypothesis that tropical soil communities are highly sensitive to warming and are consistent with independent evidence for deep evolutionary niche specialization in tropical soil microbes[32]. Further, we note that in view of the widespread evidence for intensive feedbacks among tropical soil microbial communities, plant diversity and soil processes[26,43,64], declines in microbial diversity may have substantial implications for the resilience of tropical forest functioning, composition and diversity in a warming climate. Alongside the decline in diversity observed in this experiment, the concurrent increased abundance of thermotolerant species resulted in a stable microbial biomass, accelerated enzymatic activity and increased soil CO_2 emissions. This finding partially supports previous model-based projections showing increased C loss under climate warming in this century due to adaptation of microbial growth[17]. However, our results go further by demonstrating that microbial models alone do not accurately predict the change in soil C emissions under warming in tropical ecosystems, especially at high temperatures where abiotic processes may accelerate C loss. Further study is urgently required to understand these combined biotic and abiotic controls on soil C in different tropical soils and land-use contexts, the timescales of their effects and the wider consequences of declines in soil microbial diversity for the functioning and composition of tropical forests in a warmer world.

Methods

Site and experiment. The experiment was situated in a seasonally moist lowland tropical forest on Barro Colorado Island, Panama. Within the experiment area (1 ha), the dominant tree species include *Anarcardium excelsum* and *Poulsenia armata;* a full census of tree and understory species composition in this forest is available for a nearby 50 ha forest plot in forest with similar soils, tree species and demographic composition[65]. The soils are Inceptisols (fine, isohyperthermic, Dystric Eutrudepts) that are rich in clay (~54% profile-weighted clay concentration) and secondary metal oxides. The soils developed on the volcanic facies of the Bohio Formation, a basaltic conglomerate of Oligocene age[66]. Inceptisols account for 14% of the total land area in the tropics (Ultisols and Oxisols account for 20% and 23%, respectively)[67].

The SWELTR experiment consists of 10 circular plots (five paired plots, 'warm' and 'control'). Each plot measures 5 m in diameter, with approximately 10 m between each plot-pair and a minimum of 20 m between different plot-pairs. The

experiment heated approximately 120 m^3 of soil in total (5 plots × 5 m diameter × 1.2 m depth). Temperature in the internal plot area (~3 m diameter) of each warmed plot was maintained at 4 °C above the temperature in each corresponding paired control plot on the basis of the average temperature from 0–120 cm depth at the mid-radius points in each plot. For this study, we established subplots representing a high-temperature treatment, situated in a buffer zone close to the heating cable. We therefore had two subplots per plot, situated at approximately 10 cm and 1 m distance from one of the main heating rods, representing two different levels of warming. The average warming for the low-warming subplot was 2.8 °C, and 7.9 °C for the high-warming subplot (determined at 0–10 cm soil depth), based on the difference in temperature between control plots. Thus, our study consisted of three treatments, soil at 26 ± 1 °C ('control'), 29 ± 2 °C ('+3 °C') and 34 ± 7 °C ('+8 °C'), providing a test of moderate (atmospheric warming with moderate fossil fuel emission reduction) to extreme (atmospheric warming plus deforestation) predictions of warming for tropical soils in this century[5,33]. Further information on the plot design, thermostat control and power specifications can be found in ref. [13].

Soil gas-exchange and partitioning. Soil CO_2 efflux was measured every week at four systematically distributed locations within each plot from June to September 2018 (representing the 3 °C surface soil-warming treatment), and was measured twice-weekly at two systematically distributed locations within the high-warming subplot from August to September 2018 (representing the 8 °C surface soil-warming treatment). Soil CO_2 efflux measurements were made using an infrared gas analyser (IRGA Li-8100; LI-COR Biosciences) along with measurements of soil temperature (using a HI98509 thermometer probe; Hanna Instruments) and soil moisture (using a Thetaprobe; Delta-T) at 0–20 cm soil depth for a random location immediately adjacent to each soil collar.

Soil sampling. Soil for this study was sampled during the wet season (June–Sept) in 2018. We sampled during the wet season to ensure that there was no moisture limitation to soil microbial activity and soil processes, and no difference in moisture limitation among treatments. Soil was sampled from 0–10 cm depth from the mineral horizon for each subplot and analysed for properties: total elements, available nutrients, exchangeable cations, microbial C, N and P, and enzyme activities using standard procedures (see below). We calculated microbial carbon-use-efficiency (CUE) using microbial C, N and P, and enzyme activity data using a stoichiometric method (see below). All analyses were determined on fresh soils within 24 h of sampling, except for K_2SO_4 extracts on fresh soils for which analysis was done within 6 h; growth assays on fresh soils within ~14 d; total elements (C, N, P), cations and pH on air-dried soil samples; and samples for microbial community analyses stored at −60 °C until DNA extraction. All analyses were performed on replicate soil samples ($n = 5$).

DNA extraction, sequencing and processing. DNA was extracted using the DNeasy Powersoil kit (Qiagen) and communities (bacterial and fungal) were amplified using a two-stage PCR protocol. For bacteria, we amplified the V4 hypervariable region of the 16S ribosomal RNA and for fungi we amplified the first internal transcribed spacer (ITS1) region of the rRNA operon (see Supplementary Methods for complete details). Libraries were sequenced on an Illumina MiSeq with 250 bp paired-end reads. Reads in the 16S rRNA and ITS datasets were first trimmed of forward and reverse primers. On the basis of visual inspection of read quality profiles, we removed the reverse reads from the 16S rRNA analysis due to poor quality. We then used DADA2[68] within the R environment (R Core Team, 2019) (v4.1.0) to filter and trim both datasets (on the basis of quality profiles), error correct, dereplicate and infer amplicon sequence variants (ASVs). We then merged paired-end reads (ITS only) and constructed sequence tables for both datasets. In the final step, we removed chimeras and assigned taxonomy. For a detailed description of filtering of sequencing data and workflow, including all references, see Supplementary Methods.

Soil properties. Soil microbial biomass C and N were measured by fumigation-extraction[69,70] and extractable C and N were determined by fresh soil extraction in 0.5 M K_2SO_4. Extracts were analysed for extractable organic C and N using a TOC-VCHN analyser (Shimadzu). Microbial C and N were calculated as the difference between fumigated and unfumigated extracts and corrected for unrecovered biomass using a k factor of 0.45[71]. Microbial biomass P was determined by hexanol fumigation and extraction with anion-exchange membranes[72]. Extractable P was determined using unfumigated samples and microbial P was calculated as the difference between the fumigated and unfumigated samples, with correction for unrecovered biomass using a k_p factor of 0.4[72]. Exchangeable cations were determined by extraction in 0.1 M $BaCl_2$ and detection by inductively coupled plasma-optical emission spectrometry (Optima 7300 DV; Perkin-Elmer). Effective cation exchange capacity was calculated as the sum of the charge equivalents of Al, Ca, Fe, K, Mg, Mn and Na. Soil pH was determined in deionized water in a 1:2 soil to solution ratio. All soil chemical properties were expressed on the basis of oven-dry equivalent soil (determined by drying at 105 °C for 24 h).

Soil enzymes. We determined maximum potential enzyme activity (V_{max}) and the temperature sensitivity of enzyme activity (Q_{10} of V_{max}) for 10 enzymes involved in C, N, P and S cycling. We determined V_{max} and Q_{10} of V_{max} for all treatments for in situ warmed soils (control, +3 °C and +8 °C). For the determination of Q_{10} of V_{max}, we determined V_{max} for a range of temperatures using laboratory assays.

Enzymes involved in C cycling under study were: α-glucosidase and β-glucosidase (act on α- and β-bonds in glucose, respectively), cellobiohydrolase (acts on cellulose), β-xylanase (acts on hemicellulose) and phenol oxidase (acts on phenolic compounds). Enzymes involved in P cycling: phosphomonoesterase and phosphodiesterase (acts on monoester- and diester- linked simple organic phosphates, respectively). Enzymes involved in N cycling: *N*-acetyl β-glucosaminidase (acts on *N*-glycosidic bonds) and leucine aminopeptidase (acts on amino acid leucine from proteins). Enzyme involved in S cycling: sulfatase (acts on sulfated glucosamines). For subsequent discussion, enzymes are abbreviated to: α-glucosidase (AG_{ase}), β-glucosidase (BG_{ase}), phosphodiesterase (BP_{ase}), cellobiohydrolase (CE_{ase}), leucine aminopeptidase (LP_{ase}), phosphomonoesterase (P_{ase}), *N*-acetyl β-glucosaminidase (N_{ase}), phenol oxidase (PX_{ase}), sulfatase (S_{ase}) and β-xylanase (XY_{ase}).

Hydrolytic enzymes (AG_{ase}, BG_{ase}, BP_{ase}, CE_{ase}, P_{ase}, N_{ase}, S_{ase}, XY_{ase}) were measured using microplate fluorometric assays with methylumbelliferone (MU)-linked substrates, except for LP_{ase}, which was measured using L-leucine-AMC substrate (Sigma Aldrich). PX_{ase} was measured using L-dihydroxyphenyalanine (L-DOPA) as substrate (Sigma Aldrich). Fluorimetric substrates were dissolved in 0.4% methylcellosolve (2-methoxyethanol; 0.1% final concentration in the assay). The hydrolytic fluorometric and LP_{ase} methods are based on the protocols described in refs. [73,74], while the PX_{ase} method is described in ref. [58].

For each soil sample, five replicate microplates were prepared and incubated at 2, 10, 22, 30 and 40 °C. For the fluorometric assays, 2 g fresh soil (field moist weight basis) was added to 200 ml 1 mM sodium azide (NaN_3) solution and dispersed by stirring vigorously on a magnetic stir plate. After 5 min and while stirring, 50 µl aliquots of soil suspension were removed using an 8-channel pipette and dispensed into a 96-well microplate containing 50 µl modified universal buffer solution adjusted to soil pH. Each microplate included assay wells (soil solution, buffer and 100 µl 200 µM MU substrate; 100 µM MU substrate in final solution), blank wells (soil solution, buffer and 100 µl 1 mM NaN_3) and quench wells (soil solution, buffer and 100 µl MU standard). For LP_{ase}, we used 1 mM L-leucine-AMC substrate. There were eight analytical replicate wells for each assay, and control plates for each set of assays with the standards and no soil solution (to determine fluorescence from substrates and quenching by soil solution in assay plates). Microplates were incubated at each specified temperature for 1–4 h, with incubation times based on preliminary assays for each specific substrate to assess the linearity of the reaction over time. Following incubation, 50 µl 0.5 M NaOH was added to each well for MU substrates (but not for AMC substrates) and plates were immediately analysed on a Fluostar Optima spectrofluorometer (BMG Labtech), with excitation at 360 nm and emission at 450 nm. For PX_{ase} assays, 1 g soil (oven-dry basis) was added to 100 ml 5 mM bicarbonate buffer and stirred vigorously; 100 µl 5 mM L-DOPA solution and 100 µl of soil solution were dispensed into a 96-well microplate. Control plates were made using 100 µl 5 mM bicarbonate buffer and 100 µl aliquots of soil solution. There were 16 analytical replicates and controls per soil sample. Plates were analysed on a spectrofluorometer, with PX_{ase} activity calculated as the increase in absorbance at 450 nm over 1 h. Enzyme activities were expressed on the basis of soil organic C. Hydrolytic enzyme activities, determined using MU substrates, were expressed in nmol substrate (MU or AMC) min^{-1} gC^{-1}. PX_{ase}, determined using L-DOPA as a substrate, was expressed in mg diqc h^{-1} gC^{-1} (where diqc is the L-DOPA product 3-dihydroindole-5,6-quinone-2-carboxylate).

We determined the temperature sensitivity of maximum potential enzyme activity (V_{max}) by calculating Q_{10} values as follows:

$$Q_{10} = \exp(10k), \text{ where } k = \ln\frac{V_{max}}{t},$$

where k is the exponential rate at which V_{max} increases with temperature (t)[56]. To calculate k (and thus Q_{10}), we used linear regression and included enzyme data determined between 2 °C and 40 °C. We only determined Q_{10} values of enzyme activity during the exponential increase in activity with temperature according to Arrhenius kinetics, before reaching any thermal optima of activity at which dynamics depart from Arrhenius kinetics. The thermal optima of enzymes are widely associated with enzyme denaturation that begins to occur at temperatures above 40 °C[75].

Determination of CUE. Changes in microbial community function, including growth and CUE, have been shown by models to have an extremely large influence on the soil–atmospheric C exchange and soil C storage under climatic change[17,50]. However, empirical evidence on the long-term response of microbial community physiology and its influence on soil C storage is lacking due in part to both a lack of long-term experimentation and methodological difficulties in quantifying the relevant microbial community response. Microbial CUE, for example, is an emergent property representing the ratio of C lost in respiration to C accumulated during growth[76] and can be quantified in numerous ways, including using substrate-induced respiration (^{13}C substrates)[77], ^{18}O labelling in water[78], mass-balance and the stoichiometry of enzyme activity and biomass[79]. Because it is an emergent property and therefore challenging to quantify, CUE estimates can

vary among methods and thus require interpretation that considers the method used for its quantification.

We estimated CUE on the basis of stoichiometry of enzyme activity and elemental ratios in the microbial biomass[79]. The stoichiometric method has been found to be robust and correlated with substrate-non-specific ^{18}O labelling methods[80]; it is useful because it is based on direct measurements of soil properties and can therefore be more easily compared among studies[76]. We estimated CUE from ecological stoichiometry whereby CUE is a function of the difference between its elemental requirements for growth (C, N or P in biomass and enzymatic investment for acquisition) and the abundance of environmental substrate (C, N or P in soil organic matter). This approach assumes that enzyme activities scale with microbial production and organic matter concentration, and that microbial communities exhibit optimum resource allocation with respect to enzyme expression and environmental resources; these assumptions are empirically supported by Michaelis-Menten kinetics and metabolic control analysis[79]. Based on this underlying assumption, CUE was therefore calculated as follows:[79]

$$\mathrm{CUE}_{\mathrm{C:X}} = \mathrm{CUE}_{\mathrm{MAX}}\left[\frac{S_{\mathrm{C:X}}}{(S_{\mathrm{C:X}} + K_{\mathrm{X}})}\right], \textbf{ where } S_{\mathrm{C:X}} = \left(\frac{1}{\mathrm{EEA}_{\mathrm{C:X}}}\right)\left(\frac{B_{\mathrm{C:X}}}{L_{\mathrm{C:X}}}\right)$$

where $S_{C:X}$ is a scalar that represents the extent to which the allocation of enzyme activities offsets the disparity between the elemental composition of available resources and the composition of microbial biomass; K_x and CUE_{MAX} are constants: half-saturation constant (K_x) = 0.5; and the upper limit for microbial growth efficiency based on thermodynamic constraints, CUE_{MAX} = 0.6. EEA is extracellular enzyme activity (nmol g^{-1} h^{-1}); $EEA_{C:N}$ was calculated as BG/NAG, where BG is β-glucosidase and NAG is *N*-acetyl β-glucosaminidase; and $EEA_{C:P}$ was calculated as BG/P, where P is phosphomonoesterase. Molar ratios of soil organic C:total N:total P were used as estimates of $L_{C:N}$ or $L_{C:P}$. Microbial biomass ($B_{C:X}$) C:N and C:P were also calculated as molar ratios.

Using the stoichiometric method, we found no change in CUE in this study (on 3 °C and 8 °C warming effects during the wet season; Extended Data Fig. 6), or over 2 years following 3 °C warming in surface soils[13]. However, given the apparent acceleration of enzyme activity via abiotic mechanisms (see Discussion), we suggest that this renders low confidence in the stoichiometric method in this instance, given its assumption that enzymatic activity is correlated with biological synthesis[79].

Instantaneous temperature response of microbial growth and respiration. We used the instantaneous temperature response of microbial growth and respiration to: (1) predict the effect of warming on in situ soil CO_2 emissions and (2) determine the temperature adaptation of the bacterial community following 2 years of in situ warming. For the former, we measured the instantaneous temperature response of respiration and bacterial growth for control soils only. For the latter, we measured the instantaneous temperature response of bacterial community growth for all warming treatments and controls, assuming that temperature adaptation of respiration responded similarly to bacterial growth, as found in tropical soils elsewhere[21]. To determine the temperature response of bacterial growth, we used the leucine (Leu) incorporation method;[20] for the temperature response of instantaneous respiration, we used incubation assays with measurement of headspace CO_2. Full details on these respective methods are described below.

The temperature response of bacterial community growth was determined by measuring instantaneous growth across a range of temperatures (4 to 40 °C) using the Leu-incorporation method[81]. Soil (1 g dry weight) was mixed with 20 ml 17 °C distilled water, vortexed for 3 min and centrifuged at 15 °C for 10 min. The supernatant, with an extracted bacterial suspension, was transferred (1.5 ml) into microcentrifugation vials that were pre-incubated in water baths for 0.5 to 1 h before 2 µl 3H-leucine (1-(4,5-3H) leucine, 37 MBq ml^{-1} and 5.74 TBq $mmol^{-1}$; Perkin-Elmer), together with unlabelled Leu, was added (resulting in 275 nM in the bacterial suspension). Trichloroacetic acid was added to terminate growth after 1–6.5 h, depending on incubation temperature. Measurement of radioactivity was conducted following ref. [81].

The instantaneous temperature response of respiration was determined by incubating 2 g fresh soil in 20 ml vials for 140 h (at 10 °C) or for 24 h (at 28 °C). At the end of each incubation, we sampled the vial headspace and determined the CO_2 concentration (using gas chromatography equipped with a methanizer and a flame ionization detector) to calculate the respiration rate per g soil.

To estimate the degree of microbial community adaptation to temperature, we used two complementary indices: the T_{min}[16] and the log ratio of activity at 40 °C/4 °C (temperature sensitivity index, SI)[82]. The T_{min} index provides insight on temperature adaptation across a broader temperature range and is calculated by the rate of increase in activity across temperatures from 4–28 °C. The SI index provides alternative information on the temperature adaptation of the bacterial community including also high temperatures. Because T_{min} and SI are closely related[19,20], we report both values but focus our analyses on the response of T_{min}.

Determination of T_{min} for respiration and growth and the predicted response of CO_2 efflux to in situ warming. The T_{min} of microbial activity was calculated using empirically defined microbial activity across the temperature range 4–28 °C (where the increase in the SQRT of activity is linear) according to the Ratkowsky (square root) equation:[16,18]

$$\sqrt{\mathrm{Activity}} = a\,(T - T_{\mathrm{min}})$$

where T is the measurement temperature, T_{min} is the minimum temperature for activity (temperature where activity =0) and a is empirically defined by the slope parameter from the square root of activity plotted against temperature; and where activity is either bacterial or fungal growth rates, or respiration. We determined T_{min} for each field replicate (n = 5 plots).

We then used the instantaneous temperature sensitivity of bacterial activity (T_{min}) to model the CO_2 efflux response to warming, both with and without microbial community adaptation. To model the CO_2 efflux response to warming, we used the following equation:

$$\text{Predicted } CO_2 = [a\,(T - T_{\mathrm{min}})]^2$$

where T_{min} is for control soils. To model the CO_2 efflux response to warming following temperature adaptation of microbial communities, we refitted the model using the T_{min} determined for bacterial growth in experimentally warmed soils for 2 years by 3 °C and 8 °C ('adapted' communities).

Treatment effects on soil properties. To determine treatment effects on soil CO_2 emissions, soil moisture and temperature, we used repeated measures analysis of variance (ANOVA) fitted by maximum likelihood (repeated measures model with time as random factor). To determine treatment effects (levels: control, +3 °C and +8 °C) on soil properties, we used one-way ANOVA with post-hoc Tukey honest significant difference (HSD) tests. We used this approach for all soil properties, including enzyme V_{max} and the Q_{10} of V_{max} for each enzyme determined at soil temperature. Before analyses, all data were tested for normality using a Shapiro-Wilk test and log-transformed if non-normally distributed.

Microbial community analysis. To determine temperature treatment effects on alpha diversity of soil bacterial and fungal communities, we first applied general prevalence filtering using the R package PERFect (PERmutation Filtering test for microbiome data)[83] (v0.2.4). Here we used the function PERFect_sim with the alpha parameter set to 0.05 for the 16S rRNA data and 0.1 for the ITS data. We also applied two complementary methods of prevalence filtering to determine how filtering influenced alpha diversity estimates (see Supplementary Methods for complete details). We then calculated Hill numbers using the R package hilldiv[84] (v1.5.1), specifically Observed richness (q-value = 0), Shannon exponential (q-value = 1) and Simpson multiplicative inverse (q-value = 2). We used Shapiro-Wilk normality test and Bartlett's test of homogeneity of variances to determine whether Hill numbers were normally distributed. In cases where both P values were greater than 0.05 (parametric data), we used ANOVA followed by Tukey post-hoc analysis to test for significance. For non-parametric data (cases where one or both P values were less than 0.05), we instead used Kruskal-Wallis followed by Dunn test with Benjamini-Hochberg correction.

For soil bacterial and fungal beta diversity, we calculated distance matrices for the filtered datasets using unweighted and weighted UniFrac[85] for the 16S rRNA data and Jensen-Shannon Divergence and Bray-Curtis for the ITS data. To test for temperature treatment effects on beta diversity, we used the vegan package[86] (v2.5-7) to first calculate beta dispersion for the distance matrices (betadisper function), then performed a permutation test for homogeneity of multivariate dispersions (permutest function) and finally run PERMANOVA (adonis function; assuming equal dispersion) or analysis of similarity (ANOSIM; where beta dispersion was significant).

To identify ASVs from the bacterial and fungal communities that were differentially abundant across temperature treatments, we used indicator species analysis (ISA)[87] and linear discriminant analysis (LDA) effect size (LEfSe)[88]. Before differential abundance analysis, we applied PIME (prevalence interval for microbiome evaluation)[89] (v0.1.0) filtering to both complete datasets. PIME is a slightly more aggressive filtering tool specifically designed to work with datasets containing high variation among samples[89]— a pattern observed in the +8 °C warming samples from the 16S rRNA data and all treatments from the ITS data (Extended Data Fig. 2c,f). PIME applies prevalence filtering on a per treatment basis and removes a substantial amount of within-group variation by eliminating low abundance ASVs in each treatment and retaining only those ASVs shared at the selected level of prevalence within a given treatment[89]. Following the developer's recommendation, we first rarefied all samples to even depths (per sample: 16S rRNA, 25,088 reads; ITS, 9,172 reads) and then split the datasets by predictor variable (temperature treatment) using the pime.split.by.variable function in R. Next, we calculated all prevalence intervals from 5% to 95% (increments of 5%) with the function pime.prevalence and then used the function pime.best.prevalence to choose the best prevalence. The best prevalence interval was selected when the out-of-bag error rate first reached zero or close to zero. The most prevalent ASVs (at the best prevalence interval) were retained from each split. Splits were then merged to obtain the final PIME-filtered dataset. ISA was computed with the R package 'labdsv'[90] (v2.0-1); ASVs were considered an indicator of a treatment if they had a P value less than or equal to 0.05. LEfSe

analysis was performed in the R package microbiomeMarker[91] (v0.0.1) using the following parameters: pre-sample normalization of the sum of values set to $1 \times 10^{+06}$, lda_cutoff = 2, kw_cutoff = 0.5 and wilcoxon_cutoff = 0.5. We used anvi'o[92] (v7-dev) to visualize the distribution of PIME-filtered 16S rRNA ASVs represented by more than 100 total reads and PIME-filtered ITS ASVs represented by more than 50 reads. We then overlaid the results of the ISA and LEfSe analyses. Hierarchical clustering of ASVs was performed using Euclidean distance and Ward linkage against the ASV/sample abundance matrix, while hierarchical clustering of samples was performed using Bray-Curtis distance and complete linkage.

To assess potential drivers of change in microbial community composition, we used three subsets of metadata to test correlations with community change: (1) environmental properties, (2) soil functional responses and (3) temperature adaptive responses. For each of the three metadata subsets, we performed the following steps: (1) used Shapiro-Wilk normality test to determine which metadata parameters are normally distributed; (2) used the R package bestNormalize[93] to find and execute the best normalization transformation for non-normally distributed parameters; (3) performed autocorrelation tests for all pair-wise comparisons; (4) removed autocorrelated parameters; (5) ran Mantel tests to determine whether any of the metadata subsets is significantly correlated with microbial community data; and (6) used the bioenv function (vegan package) to identify metadata parameters that are most strongly correlated with the community data. In last step, (7) we performed distance-based redundancy analysis (db-RDA) using capscale from the vegan package. First, we ran rankindex (vegan) to select the best community dissimilarity index. Then, we ran capscale for db-RDA. Next, we used envfit (vegan) to fit environmental parameters onto ordinations. Finally, we selected all metadata parameters that were significant for bioenv (see above) and/or envfit analyses for plotting the ordinations and vector overlays. For a detailed description of community analyses, including all references, see Supplementary Methods.

Reporting summary. Further information on research design is available in the Nature Research Reporting Summary linked to this article.

Data availability

Trimmed (primers removed) sequence data generated in this study are deposited in the European Nucleotide Archive (ENA) under Project Accession number PRJEB45074 (ERP129199), sample accession numbers ERS6485270–ERS6485284 (16S rRNA) and sample accession numbers ERS6485285–ERS6485299 (ITS). Raw fastq files can be accessed through the Smithsonian figshare at https://doi.org/10.25573/data.14686665 (16S rRNA) and https://doi.org/10.25573/data.14686755 (ITS). Related data and data products for individual analysis workflows are available through the Smithsonian figshare under the collection https://doi.org/10.25573/data.c.5667571.

Code availability

All code, reproducible workflows and further information on data availability can be found on the project website at https://sweltr.github.io/high-temp/. The code embedded in the website is available on GitHub (https://github.com/sweltr/high-temp/) in R Markdown format. The version of code used in this study is archived under SWELTR Workflows v1.0 (https://github.com/sweltr/high-temp), DOI identifier https://zenodo.org/badge/latestdoi/368915237.

Received: 17 November 2021; Accepted: 12 July 2022;
Published online: 05 September 2022

References

1. Cavicchioli, R. et al. Scientists' warning to humanity: microorganisms and climate change. *Nat. Rev. Microbiol.* **17**, 569–586 (2019).
2. Jackson, R. B. et al. The ecology of soil carbon: pools, vulnerabilities, and biotic and abiotic controls. *Annu. Rev. Ecol. Evol. Syst.* **48**, 419–445 (2017).
3. Pan, Y. et al. A large and persistent carbon sink in the world's forests. *Science* **333**, 988–993 (2011).
4. Myers, N., Mittermeier, R. A., Mittermeier, C. G., da Fonseca, G. A. B. & Kent, J. Biodiversity hotspots for conservation priorities. *Nature* **403**, 853–858 (2000).
5. IPCC. *Climate Change 2021: The Physical Science Basis.* (eds Masson-Delmotte, V. et al.) (Cambridge Univ. Press, in press).
6. Mora, C. et al. The projected timing of climate departure from recent variability. *Nature* **502**, 183–187 (2013).
7. Wood, T. E. et al. in *Ecosystem Consequences of Soil Warming: Microbes, Vegetation, Fauna and Soil Biogeochemistry* (ed. Mohan, J.) Ch. 14 (Academic Press, 2019).
8. Davidson, E. A. & Janssens, I. A. Temperature sensitivity of soil carbon decomposition and feedbacks to climate change. *Nature* **440**, 165–173 (2006).
9. van Gestel, N. et al. Predicting soil carbon loss with warming. *Nature* **554**, E4–E5 (2018).
10. Melillo, J. M. et al. Long-term pattern and magnitude of soil carbon feedback to the climate system in a warming world. *Science* **358**, 101–104 (2017).
11. Romero-Olivares, A. L., Allison, S. D. & Treseder, K. K. Soil microbes and their response to experimental warming over time: a meta-analysis of field studies. *Soil Biol. Biochem.* **107**, 32–40 (2017).
12. Anderson-Teixeira, K. J., Wang, M. M. H., McGarvey, J. C. & LeBauer, D. S. Carbon dynamics of mature and regrowth tropical forests derived from a pantropical database (TropForC-db). *Glob. Change Biol.* **22**, 1690–1709 (2016).
13. Nottingham, A. T., Meir, P., Velasquez, E. & Turner, B. L. Soil carbon loss by experimental warming in a tropical forest. *Nature* **584**, 234–237 (2020).
14. Kimball, B. A. et al. Infrared heater system for warming tropical forest understory plants and soils. *Ecol. Evol.* **8**, 1932–1944 (2018).
15. DeAngelis, K. M. et al. Long-term forest soil warming alters microbial communities in temperate forest soils. *Front. Microbiol.* https://doi.org/10.3389/fmicb.2015.00104 (2015)
16. Bååth, E. Temperature sensitivity of soil microbial activity modeled by the square root equation as a unifying model to differentiate between direct temperature effects and microbial community adaptation. *Glob. Change Biol.* **24**, 2850–2861 (2018).
17. Wieder, W. R., Bonan, G. B. & Allison, S. D. Global soil carbon projections are improved by modelling microbial processes. *Nat. Clim. Change* **3**, 909–912 (2013).
18. Ratkowsky, D. A., Olley, J., Mcmeekin, T. A. & Ball, A. Relationship between temperature and growth-rate of bacterial cultures. *J. Bacteriol.* **149**, 1–5 (1982).
19. Rinnan, R., Rousk, J., Yergeau, E., Kowalchuk, G. A. & Bååth, E. Temperature adaptation of soil bacterial communities along an Antarctic climate gradient: predicting responses to climate warming. *Glob. Change Biol.* **15**, 2615–2625 (2009).
20. Nottingham, A. T., Bååth, E., Reischke, S., Salinas, N. & Meir, P. Adaptation of soil microbial growth to temperature: using a tropical elevation gradient to predict future changes. *Glob. Change Biol.* https://doi.org/10.1111/gcb.14502 (2019).
21. Li, J. Q., Bååth, E., Pei, J. M., Fang, C. M. & Nie, M. Temperature adaptation of soil microbial respiration in alpine, boreal and tropical soils: an application of the square root (Ratkowsky) model. *Glob. Change Biol.* **27**, 1281–1292 (2021).
22. Rousk, J., Frey, S. D. & Bååth, E. Temperature adaptation of bacterial communities in experimentally warmed forest soils. *Glob. Change Biol.* **18**, 3252–3258 (2012).
23. Nottingham, A. T. et al. Annual to decadal temperature adaptation of the soil bacterial community after translocation across an elevation gradient in the Andes. *Soil Biol. Biochem.* **158**, 108217 (2021).
24. Nottingham, A. T. et al. Microbial responses to warming enhance soil carbon loss following translocation across a tropical forest elevation gradient. *Ecol. Lett.* **22**, 1889–1899 (2019).
25. Donhauser, J., Niklaus, P. A., Rousk, J., Larose, C. & Frey, B. Temperatures beyond the community optimum promote the dominance of heat-adapted, fast growing and stress resistant bacteria in alpine soils. *Soil Biol. Biochem.* **148**, 107873 (2020).
26. Mangan, S. A. et al. Negative plant–soil feedback predicts tree-species relative abundance in a tropical forest. *Nature* **466**, 752–755 (2010).
27. Pold, G., Melillo, J. M. & DeAngelis, K. M. Two decades of warming increases diversity of a potentially lignolytic bacterial community. *Front. Microbiol.* https://doi.org/10.3389/fmicb.2015.00480 (2015).
28. Zhou, J. Z. et al. Temperature mediates continental-scale diversity of microbes in forest soils. *Nat. Commun.* **7**, 12083 (2016).
29. Tedersoo, L. et al. Global diversity and geography of soil fungi. *Science* **346**, 1256688 (2014).
30. Wu, L. et al. Reduction of microbial diversity in grassland soil is driven by long-term climate warming. *Nat. Microbiol.* **7**, 1054–1062 (2022).
31. Oliverio, A. M., Bradford, M. A. & Fierer, N. Identifying the microbial taxa that consistently respond to soil warming across time and space. *Glob. Change Biol.* **23**, 2117–2129 (2017).
32. Bahram, M. et al. Structure and function of the global topsoil microbiome. *Nature* **560**, 233–237 (2018).
33. Spracklen, D. V., Baker, J. C. A., Garcia-Carreras, L. & Marsham, J. H. The effects of tropical vegetation on rainfall. *Annu. Rev. Env. Resour.* **43**, 193–218 (2018).
34. Bradford, M. A. Thermal adaptation of decomposer communities in warming soils. *Front. Microbiol.* https://doi.org/10.3389/Fmicb.2013.00333 (2013).
35. Pietikäinen, J., Pettersson, M. & Bååth, E. Comparison of temperature effects on soil respiration and bacterial and fungal growth rates. *FEMS Microbiol. Ecol.* **52**, 49–58 (2005).
36. Mori, A. S. et al. Biodiversity–productivity relationships are key to nature-based climate solutions. *Nat. Clim. Change* **11**, 543–550 (2021).
37. Delgado-Baquerizo, M. et al. Multiple elements of soil biodiversity drive ecosystem functions across biomes. *Nat. Ecol. Evol.* **4**, 210–220 (2020).

38. Wagg, C., Bender, S. F., Widmer, F. & van der Heijden, M. G. A. Soil biodiversity and soil community composition determine ecosystem multifunctionality. *Proc. Natl Acad. Sci. USA* **111**, 5266–5270 (2014).
39. Nottingham, A. T. et al. Microbes follow Humboldt: temperature drives plant and soil microbial diversity patterns from the Amazon to the Andes. *Ecology* **99**, 2455–2466 (2018).
40. Brown, J. H., Gillooly, J. F., Allen, A. P., Savage, V. M. & West, G. B. Toward a metabolic theory of ecology. *Ecology* **85**, 1771–1789 (2004).
41. Brown, J. H. Why are there so many species in the tropics? *J. Biogeogr.* **41**, 8–22 (2014).
42. LaManna, J. A. et al. Plant diversity increases with the strength of negative density dependence at the global scale. *Science* **356**, 1389–1392 (2017).
43. Bagchi, R. et al. Pathogens and insect herbivores drive rainforest plant diversity and composition. *Nature* **506**, 85–88 (2014).
44. Lapebie, P., Lombard, V., Drula, E., Terrapon, N. & Henrissat, B. Bacteroidetes use thousands of enzyme combinations to break down glycans. *Nat. Commun.* https://doi.org/10.1038/s41467-019-10068-5 (2019).
45. Makhalanyane, T. P. et al. Microbial ecology of hot desert edaphic systems. *FEMS Microbiol. Rev.* **39**, 203–221 (2015).
46. Aydogan, E. L., Moser, G., Muller, C., Kampfer, P. & Glaeser, S. P. Long-term warming shifts the composition of bacterial communities in the phyllosphere of *Galium album* in a permanent grassland field-experiment. *Front. Microbiol.* https://doi.org/10.3389/fmicb.2018.00144 (2018).
47. Hu, D. Y., Zang, Y., Mao, Y. J. & Gao, B. L. Identification of molecular markers that are specific to the class thermoleophilia. *Front. Microbiol.* https://doi.org/10.3389/fmicb.2019.01185 (2019).
48. Mohan, J. E. et al. Mycorrhizal fungi mediation of terrestrial ecosystem responses to global change: mini-review. *Fungal Ecol.* **10**, 3–19 (2014).
49. Manzoni, S., Taylor, P., Richter, A., Porporato, A. & Agren, G. I. Environmental and stoichiometric controls on microbial carbon-use efficiency in soils. *New Phytol.* **196**, 79–91 (2012).
50. Allison, S. D., Wallenstein, M. D. & Bradford, M. A. Soil-carbon response to warming dependent on microbial physiology. *Nat. Geosci.* **3**, 336–340 (2010).
51. Reed, S. C. et al. Soil biogeochemical responses of a tropical forest to warming and hurricane disturbance. *Adv. Ecol. Res.* **62**, 225–252 (2020).
52. Nottingham, A. T., Turner, B. L., Stott, A. W. & Tanner, E. V. J. Nitrogen and phosphorus constrain labile and stable carbon turnover in lowland tropical forest soils. *Soil Biol. Biochem.* **80**, 26–33 (2015).
53. Walker, T. W. N. et al. Microbial temperature sensitivity and biomass change explain soil carbon loss with warming. *Nat. Clim. Change* **8**, 885–889 (2018).
54. Kemmitt, S. J. et al. Mineralization of native soil organic matter is not regulated by the size, activity or composition of the soil microbial biomass—a new perspective. *Soil Biol. Biochem.* **40**, 61–73 (2008).
55. Nannipieri, P., Trasar-Cepeda, C. & Dick, R. P. Soil enzyme activity: a brief history and biochemistry as a basis for appropriate interpretations and meta-analysis. *Biol. Fert. Soils* **54**, 11–19 (2018).
56. Wallenstein, M., Allison, S., Ernakovich, J., Steinweg, J. M. & Sinsabaugh, R. in *Soil Enzymology.* Soil Biology Vol. 22 (eds Shukla, G. & Varma, A.) Ch. 13 (Springer, 2011).
57. Zhou, X. Y., Chen, L., Xu, J. M. & Brookes, P. C. Soil biochemical properties and bacteria community in a repeatedly fumigated-incubated soil. *Biol. Fert. Soils* **56**, 619–631 (2020).
58. Sanchez-Julia, M. & Turner, B. L. Abiotic contribution to phenol oxidase activity across a manganese gradient in tropical forest soils. *Biogeochemistry* https://doi.org/10.1007/s10533-021-00764-0 (2021).
59. Razavi, B. S., Liu, S. B. & Kuzyakov, Y. Hot experience for cold-adapted microorganisms: temperature sensitivity of soil enzymes. *Soil Biol. Biochem.* **105**, 236–243 (2017).
60. Pinney, M. M. et al. Parallel molecular mechanisms for enzyme temperature adaptation. *Science* **371**, eaay2784 (2021).
61. Fanin, N. et al. Soil enzymes in response to climate warming: mechanisms and feedbacks. *Funct. Ecol.* https://doi.org/10.1111/1365-2435.14027 (2022).
62. Hall, S. J. & Silver, W. L. Iron oxidation stimulates organic matter decomposition in humid tropical forest soils. *Glob. Change Biol.* **19**, 2804–2813 (2013).
63. Freeman, C., Ostle, N. & Kang, H. An enzymic 'latch' on a global carbon store. *Nature* **409**, 149 (2001).
64. Sarmiento, C. et al. Soilborne fungi have host affinity and host-specific effects on seed germination and survival in a lowland tropical forest. *Proc. Natl Acad. Sci. USA* **114**, 11458–11463 (2017).
65. Condit, R., Perez, R., Lao, S., Aguilar, S. & Hubbell, S. P. Demographic trends and climate over 35 years in the Barro Colorado 50 ha plot. *For. Ecosyst.* https://doi.org/10.1186/s40663-017-0103-1 (2017).
66. Woodring, W. P. Geology of Barro Colorado Island. *Smithson. Misc. Collect.* **135**, 1–39 (1958).
67. Sanchez, P. A. & Logan, T. J. Myths and science about the chemistry and fertility of soils in the tropics. *SSSA Spec. Publ.* **29**, 35–46 (1992).
68. Callahan, B. J. et al. DADA2: high-resolution sample inference from Illumina amplicon data. *Nat. Methods* **13**, 581–583 (2016).
69. Brookes, P. C., Landman, A., Pruden, G. & Jenkinson, D. S. Chloroform fumigation and the release of soil nitrogen: a rapid direct extraction method to measure microbial biomass nitrogen in soil. *Soil Biol. Biochem.* **17**, 837–842 (1985).
70. Vance, E. D., Brookes, P. C. & Jenkinson, D. S. An extraction method for measuring soil microbial biomass C. *Soil Biol. Biochem.* **19**, 703–707 (1987).
71. Jenkinson, D. S., Brookes, P. C. & Powlson, D. S. Measuring soil microbial biomass. *Soil Biol. Biochem.* **36**, 5–7 (2004).
72. Kouno, K., Tuchiya, Y. & Ando, T. Measurement of soil microbial biomass phosphorus by an anion-exchange membrane method. *Soil Biol. Biochem.* **27**, 1353–1357 (1995).
73. Tabatabai, M. A. in *Methods of Soil Analysis. Part 2. Microbiological and Biochemical Properties* (ed. Page, A.L.) 778–833 (SSSA, 1994).
74. Marx, M. C., Wood, M. & Jarvis, S. C. A microplate fluorimetric assay for the study of enzyme diversity in soils. *Soil Biol. Biochem.* **33**, 1633–1640 (2001).
75. Price, N. & Stevens, L. *Fundamentals of Enzymology: Cell and Molecular Biology of Catalytic Proteins* (Oxford Univ. Press, 1999).
76. Hagerty, S. B., Allison, S. D. & Schimel, J. P. Evaluating soil microbial carbon use efficiency explicitly as a function of cellular processes: implications for measurements and models. *Biogeochemistry* **140**, 269–283 (2018).
77. Frey, S. D., Lee, J., Melillo, J. M. & Six, J. The temperature response of soil microbial efficiency and its feedback to climate. *Nat. Clim. Change* **3**, 395–398 (2013).
78. Spohn, M. et al. Soil microbial carbon use efficiency and biomass turnover in a long-term fertilization experiment in a temperate grassland. *Soil Biol. Biochem.* **97**, 168–175 (2016).
79. Sinsabaugh, R. L. et al. Stoichiometry of microbial carbon use efficiency in soils. *Ecol. Monogr.* **86**, 172–189 (2016).
80. Geyer, K. M., Dijkstra, P., Sinsabaugh, R. & Frey, S. D. Clarifying the interpretation of carbon use efficiency in soil through methods comparison. *Soil Biol. Biochem.* **128**, 79–88 (2019).
81. Bååth, E., Pettersson, M. & Söderberg, K. H. Adaptation of a rapid and economical microcentrifugation method to measure thymidine and leucine incorporation by soil bacteria. *Soil Biol. Biochem.* **33**, 1571–1574 (2001).
82. Bárcenas-Moreno, G., Gomez-Brandon, M., Rousk, J. & Bååth, E. Adaptation of soil microbial communities to temperature: comparison of fungi and bacteria in a laboratory experiment. *Glob. Change Biol.* **15**, 2950–2957 (2009).
83. Smirnova, E., Huzurbazar, S. & Jafari, F. PERFect: PERmutation Filtering test for microbiome data. *Biostatistics* **20**, 615–631 (2019).
84. Alberdi, A. & Gilbert, M. T. P. hilldiv: an R package for the integral analysis of diversity based on Hill numbers. Preprint at *bioRxiv* https://doi.org/10.1101/545665 (2019).
85. Lozupone, C., Lladser, M. E., Knights, D., Stombaugh, J. & Knight, R. UniFrac: an effective distance metric for microbial community comparison. *ISME J.* **5**, 169–172 (2011).
86. Oksanen, J. et al. vegan: Community ecology package, R Package version 2 https://cran.r-project.org/web/packages/vegan/ (2018).
87. Dufrene, M. & Legendre, P. Species assemblages and indicator species: the need for a flexible asymmetrical approach. *Ecol. Monogr.* **67**, 345–366 (1997).
88. Segata, N. et al. Metagenomic biomarker discovery and explanation. *Genome Biol.* https://doi.org/10.1186/gb-2011-12-6-r60 (2011).
89. Roesch, L. F. W. et al. PIME: a package for discovery of novel differences among microbial communities. *Mol. Ecol. Resour.* **20**, 415–428 (2020).
90. Roberts, D.W. labdsv: Ordination and multivariate analysis for ecology. R package version 2.0-1 https://cran.r-project.org/web/packages/labdsv/ (2019).
91. Cao, Y. et al. microbiomeMarker: an R/Bioconductor package for microbiome marker identification and visualization. *Bioinformatics* **38**, 4027–4029 (2022).
92. Eren, A. M. et al. Anvi'o: an advanced analysis and visualization platform for 'omics data. *Peerj* **3**, e1319 (2015).
93. Peterson, R. A. & Cavanaugh, J. E. Ordered quantile normalization: a semiparametric transformation built for the cross-validation era. *J. Appl. Stat.* **47**, 2312–2327 (2020).

Acknowledgements

This study was supported by three fellowships to A.T.N.: UK NERC grant NE/T012226, European Union Marie-Curie Fellowship FP7-2012-329360 and an STRI Tupper Fellowship. Further support came from UK NERC grant NE/K01627X/1 to P.M., an ANU Biology Innovation grant to P.M. and Simons Foundation grant No. 429440 to W. Wcislo, STRI, and support from the US Department of Agriculture (USDA), Agricultural Research Service to K.B. We thank O. Acevado, D. Agudo, A. Bielnicka, G. Broders, M. Cano, D. Dominguez, M. Garcia, M. Larsen, J. Rodriguez, H. Szczygiel, I. Torres, E. Velasquez, W. Wcislo, K. Winter and J. Wright for support. We thank B. Turner for his contribution to SWELTR, especially during its initial phase of operation. Sequencing analyses were conducted on the Smithsonian High-Performance Cluster (SI/HPC), Smithsonian Institution (https://doi.org/10.25572/SIHPC). For the purpose of open access, the authors have applied a Creative Commons Attribution (CC BY) licence to any author-accepted manuscript version arising from this submission.

Mention of trade names or commercial products in this publication is solely for the purpose of providing specific information and does not imply recommendation or endorsement by the USDA. The USDA is an equal opportunity provider and employer.

Author contributions

A.T.N. conceived the study. A.T.N., J.J.S., M.M.-S., J.P., E.B., K.B. and K.S. performed the study. A.T.N. and J.J.S. analysed the data. A.T.N. wrote the paper with input from J.J.S., E.B., K.S., K.B. and P.M.

Competing interests

The authors declare no competing interests.

Additional information

Extended data is available for this paper at https://doi.org/10.1038/s41564-022-01200-1.

Supplementary information The online version contains supplementary material available at https://doi.org/10.1038/s41564-022-01200-1.

Correspondence and requests for materials should be addressed to Andrew T. Nottingham.

Peer review information *Nature Microbiology* thanks Nadia Maaroufi, Ashish Malik and the other, anonymous, reviewer(s) for their contribution to the peer review of this work.

Reprints and permissions information is available at www.nature.com/reprints.

Publisher's note Springer Nature remains neutral with regard to jurisdictional claims in published maps and institutional affiliations.

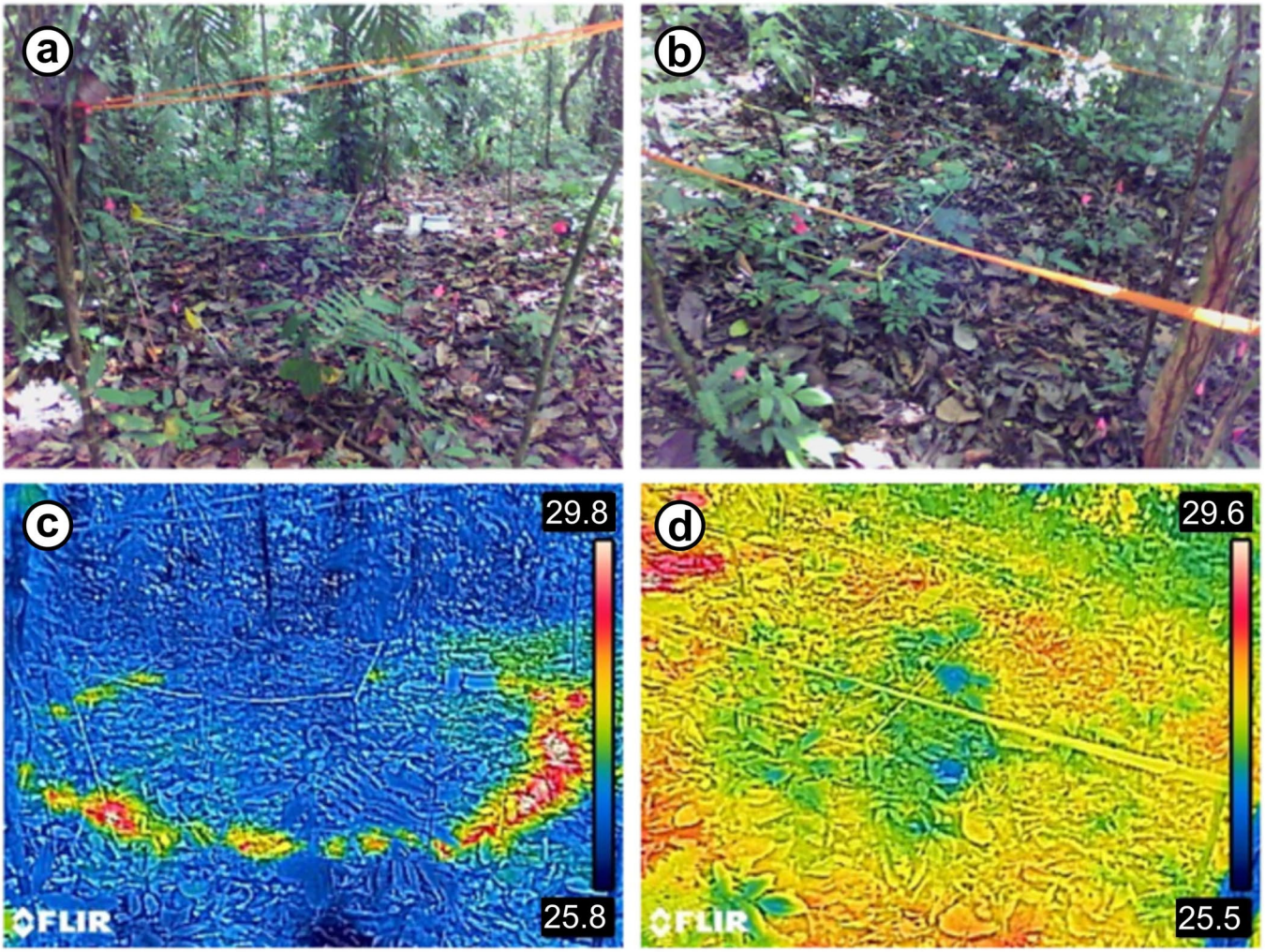

Extended Data Fig. 1 | One of five warmed plots at SWELTR. The images show the soil surface temperature shortly after the warming structure was switched on (**a** and **c**) and after a period of thermal equilibration' (**b** and **d**). The circular heating structure was 3.5 m in diameter and extended to 1.2 m depth, which resulted in an effective heated plot of approximately 5 m diameter x > 1.5 m depth (that is to the bedrock, situated at around 1.5–2.0 m across the study site). The experiment consisted of five warmed and control plot-pairs in total. For this study we had three treatment levels, +3 °C warming (within the warmed plots), +8 °C (within a high-temperature buffer zone close [~10 cm] to the heating source for each warmed plot) and ambient temperature controls (within the control plots). Therefore, all analyses are for n = 5 independent sampling locations for each treatment level. Image credit: J. Bujan and E. Velasquez.

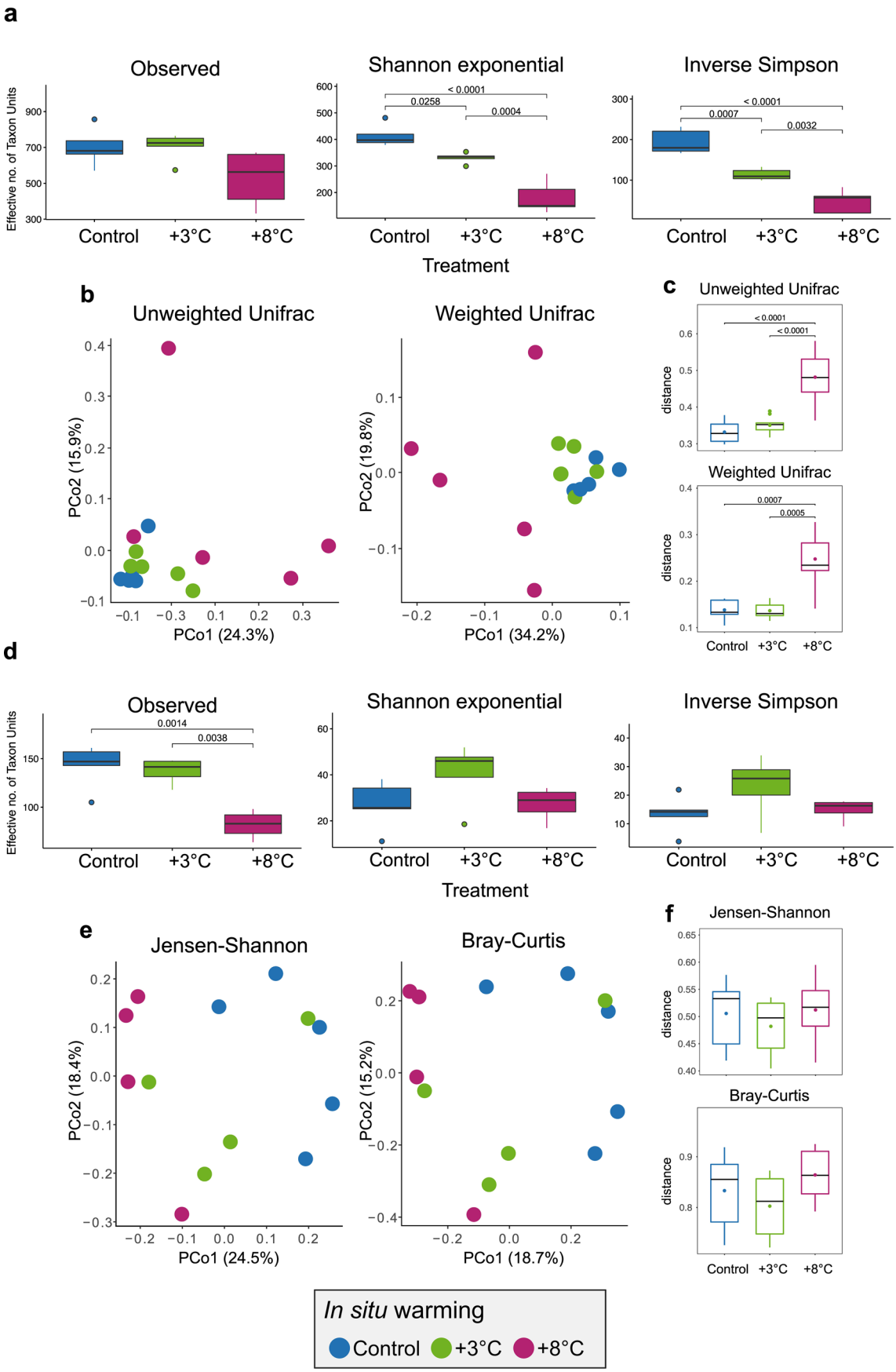

Extended Data Fig. 2 | See next page for caption.

Extended Data Fig. 2 | Diversity response of soil bacteria (a–c) and fungi (d–f) to two years of warming by +3 °C and +8 °C. Shapiro-Wilk Normality and Bartlett tests indicated all alpha diversity estimates (following PERfect filtering) were normally distributed and differences were assessed for (**a**) bacteria and (**d**) fungi using analysis of variance (ANOVA) followed by Tukey HSD post-hoc tests. Compositional similarity of microbial communities (beta-diversity) represented as PCoA ordination plots of PERfect filtered data for (**b**) bacteria—estimated using Unweighted (left) and Weighted Unifrac (right) distance matrices; and (**e**) fungi estimated—using Jensen–Shannon divergence (left) and Bray-Curtis (right) distance matrices. Within group distances for the (**c**) bacteria and (f) fungi datasets. The centre line of each box plot represents the median, the lower and upper hinges represent the first and third quartiles and whiskers represent + 1.5 the interquartile range. For panels (**a**), (**c**), (**d**), and (**f**), only significant differences between treatments are shown.

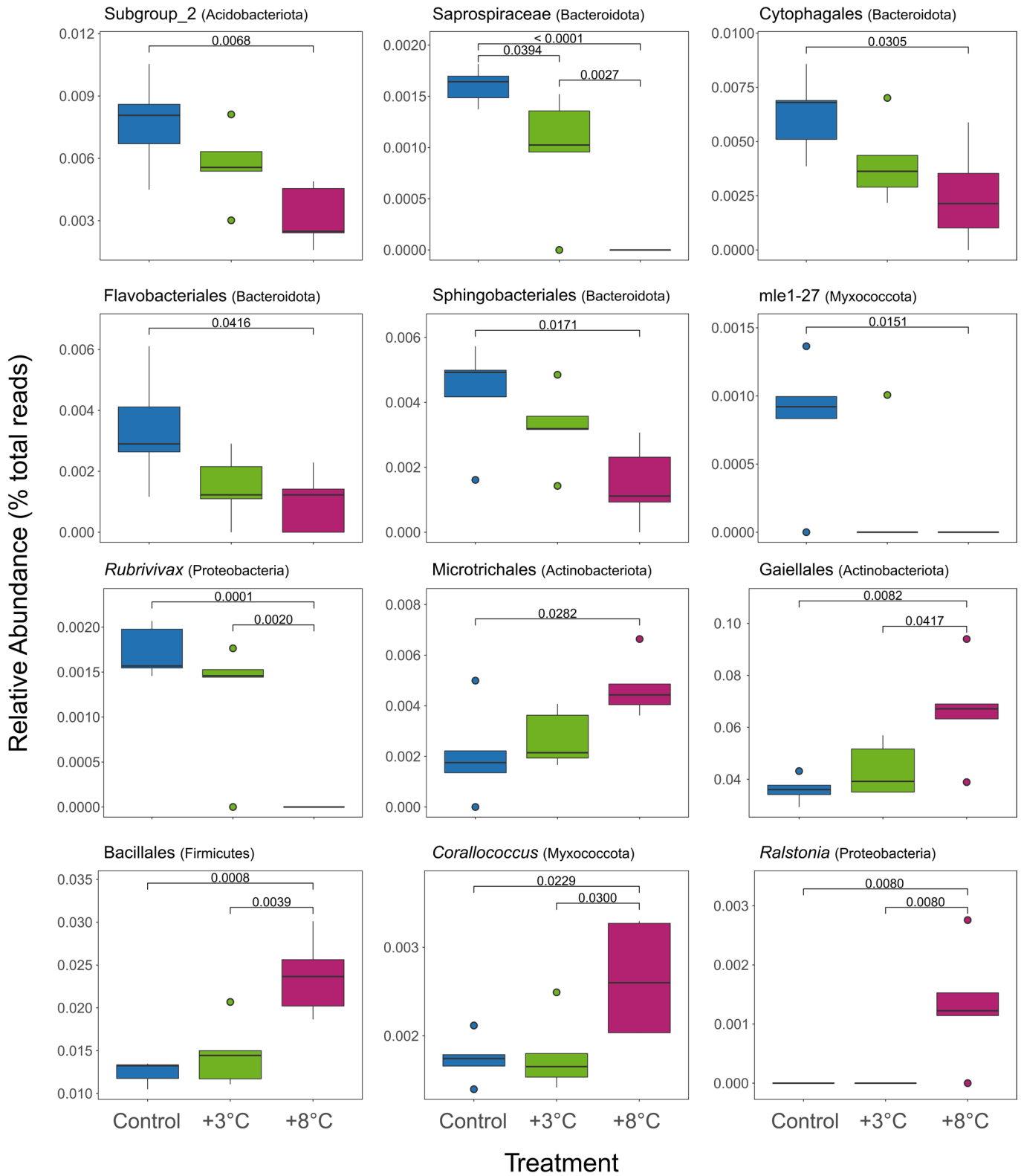

Extended Data Fig. 3 | The response of select soil bacteria taxa to two years of warming by +3 °C and +8 °C. Differences assessed for multiple-group pair-wise comparisons using ANOVA followed by Tukey HSD post hoc tests. PERfect filtered read count data was log10 transformed and normalized using total sum scaling (TSS). The centre line of each box plot represents the median, the lower and upper hinges represent the first and third quartiles and whiskers represent + 1.5 the interquartile range. Only significant differences between treatments are shown.

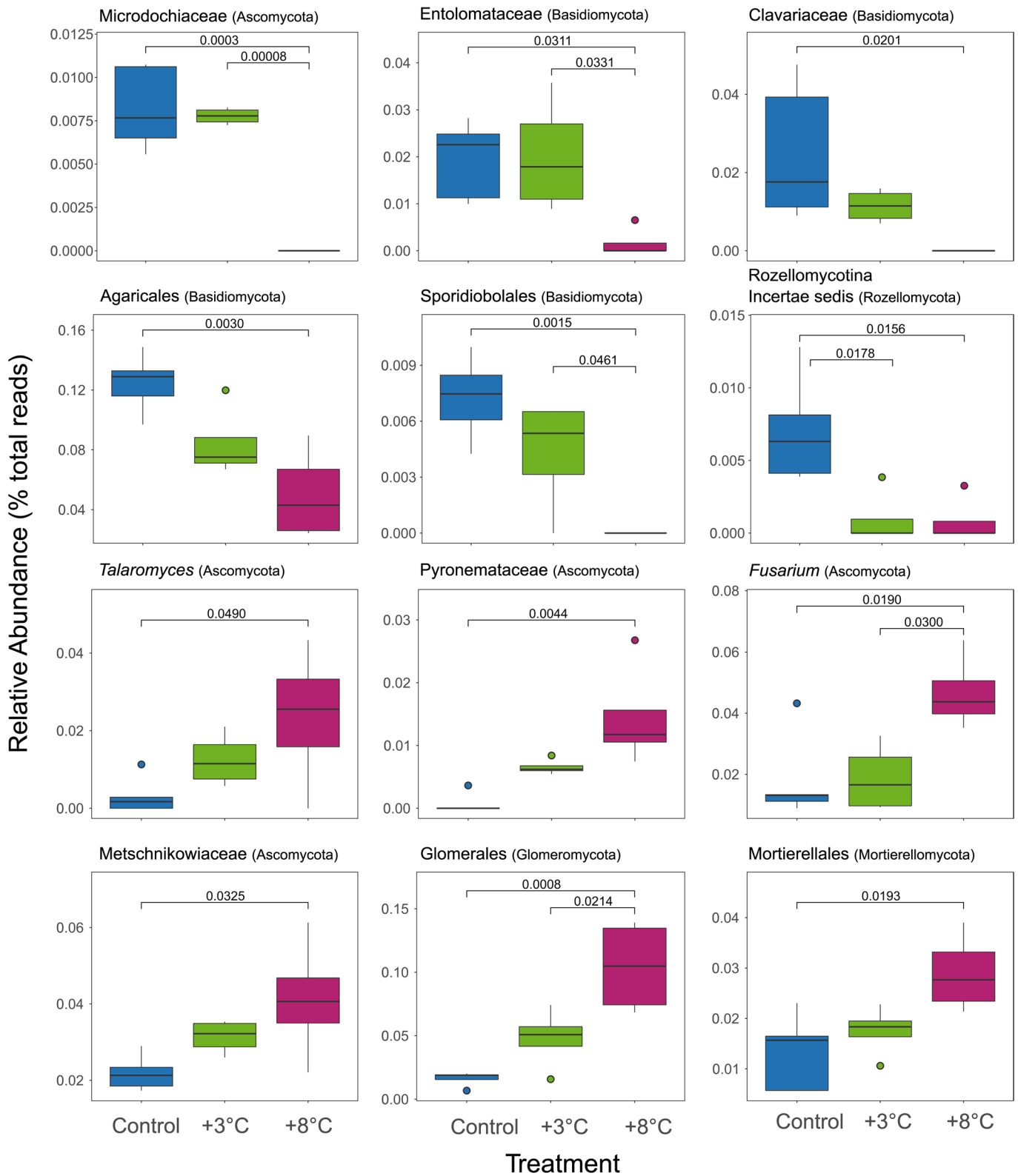

Extended Data Fig. 4 | The response of select soil fungal taxa to two years of warming by +3 °C and +8 °C. Differences assessed for multiple-group pair-wise comparisons using ANOVA followed by Tukey HSD post hoc tests. PERfect filtered read count data was log10 transformed and normalized using total sum scaling (TSS). The centre line of each box plot represents the median, the lower and upper hinges represent the first and third quartiles and whiskers represent + 1.5 the interquartile range. Only significant differences between treatments are shown.

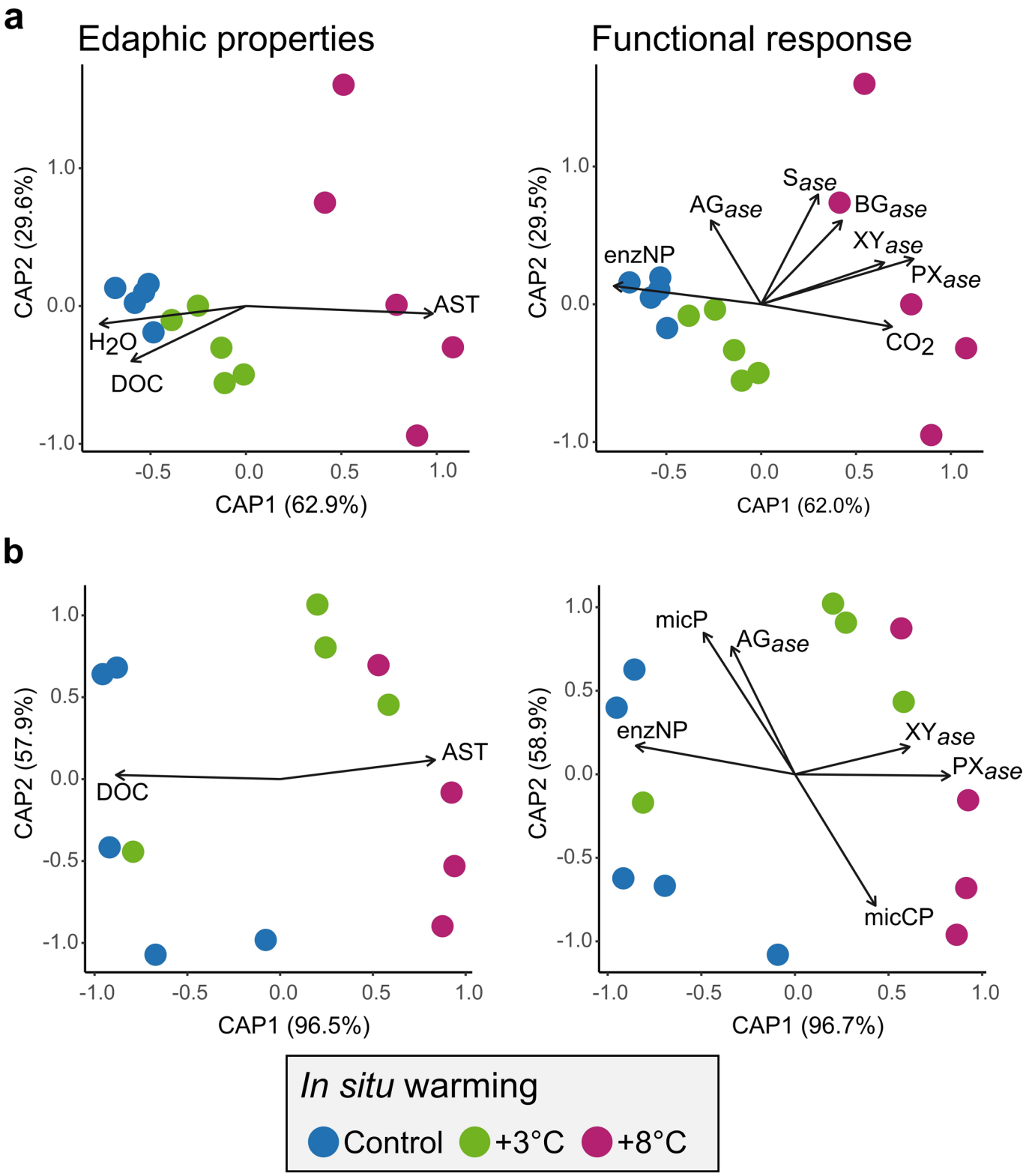

Extended Data Fig. 5 | Distance-based Redundancy Analysis (db-RDA). Distance-based Redundancy Analysis (db-RDA) of PIME filtered data based on Bray-Curtis dissimilarity showing the relationships between community composition change for (**a**) bacteria and (**b**) fungi versus edaphic properties (left) and microbial functional response (right). All analyses are for soil collected from n = 5 independent sampling locations for each treatment level.

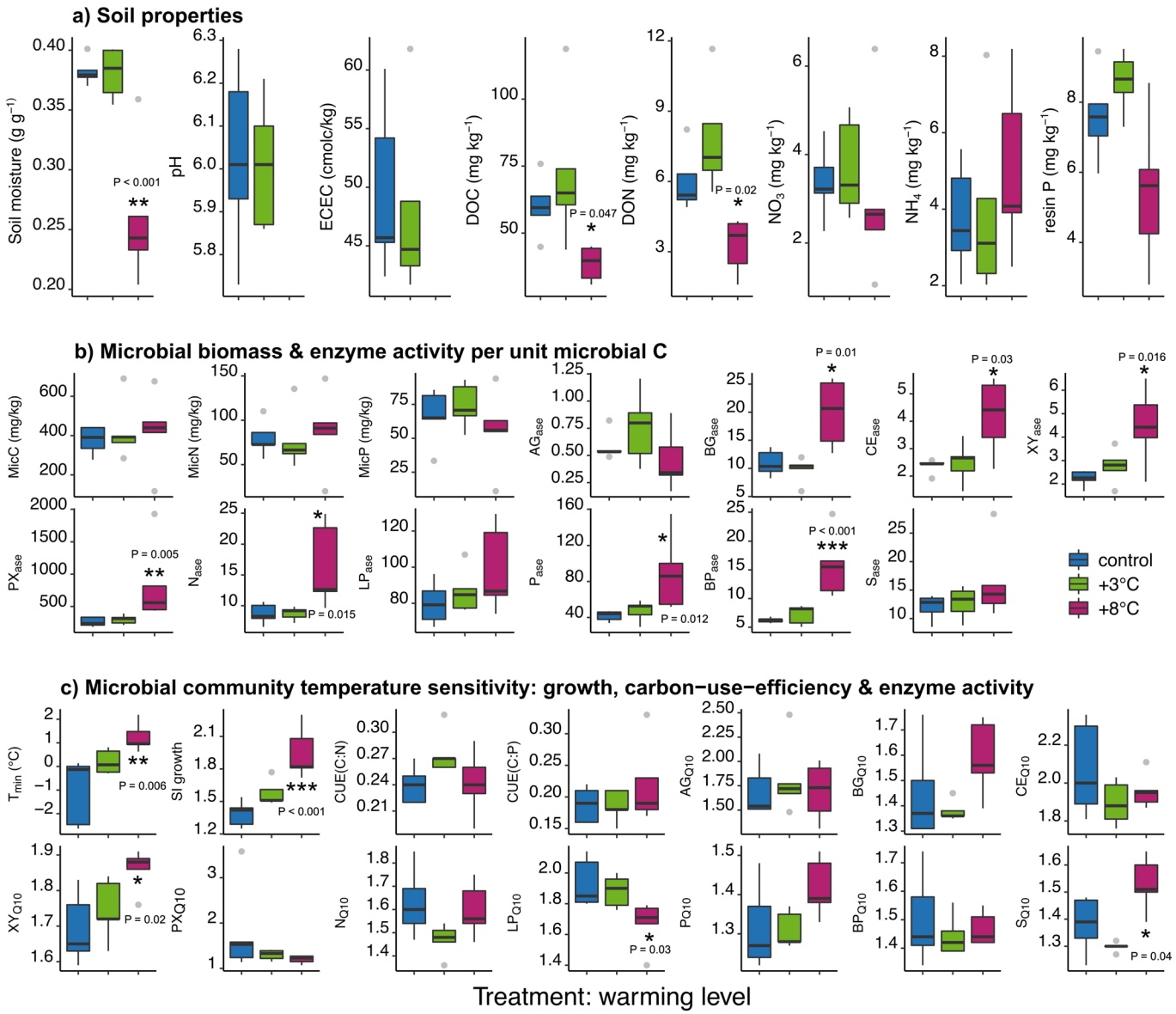

Extended Data Fig. 6 | Soil, enzyme, and microbial responses to +3 °C and +8 °C in situ soil warming. Data are grouped by (**a**) soil properties, (**b**) microbial functional responses, and (**c**) microbial temperature adaptive responses; we used the same grouping to test three hypotheses on how each of these responses were correlated to changes in microbial diversity and community composition (Fig. 2; Extended Data Table 2, Fig. 5). All properties were determined for soil samples collected during the 2018 wet season (June and November); see methods. Units for enzyme V_{max} are nmol MU g^{-1} min^{-1}, except Phenol oxidase in μmol g^{-1} h^{-1} and Leucine aminopeptidase in nmol AMC g^{-1} min^{-1}. The centre line of each box plot represents the median, the lower and upper hinges represent the first and third quartiles and whiskers represent + 1.5 the interquartile range. Significant differences between treatments and controls are highlighted by asterisks (ANOVA; * $p \leq 0.05$, ** $p \leq 0.01$, *** $p \leq 0.001$). All analyses are for soil collected from n = 5 independent sampling locations for each treatment level.

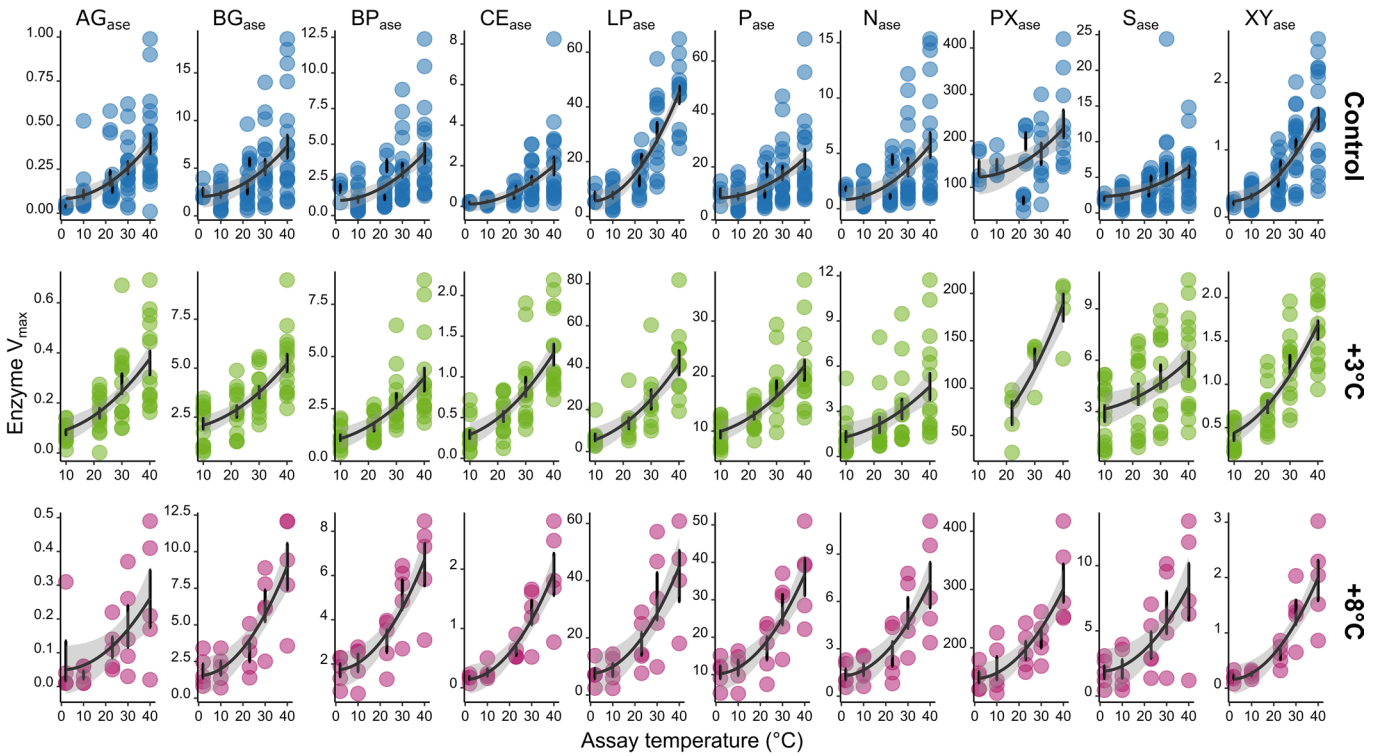

Extended Data Fig. 7 | Soil enzyme activities in response to incubation temperature (that is instantaneous temperature response determined in laboratory assays). Data are maximum potential enzyme activity (V_{max}), determined by activity under saturating substrate conditions. Enzymes are: α-glucosidase (AG_{ase}), β-glucosidase (BG_{ase}), phospho-diesterase (BP_{ase}), cellolbiohydrolase (CE_{ase}), leucine aminopeptidase (LP_{ase}), phosphomonoesterase (P_{ase}), *N*-acetyl β-glucosaminidase (N_{ase}), phenol oxidase (PX_{ase}), sulfatase (S_{ase}) and β-xylanase (XY_{ase}). Units for enzyme V_{max} are nmol MU g^{-1} min^{-1}, except Phenol oxidase in μmol g^{-1} h^{-1} and Leucine aminopeptidase in nmol AMC g^{-1} min^{-1}. The error bars represent mean ± one standard error, for n = 5 plots. Fitted lines depict quadratic functions with 95% confidence intervals. All analyses are for soil collected from n = 5 independent sampling locations for each treatment level. Activity was determined during the wet season 2018 for the following sampling periods: controls include 4 sampling periods (June, Sept, Oct, Dec 2018); +3 °C include 3 sampling periods (June, Sept, Dec 2018); +8 °C include 1 sampling period (Sept 2018).

Extended Data Table 1 | Relationship of bacterial and fungal richness with (a) environmental drivers, (b) microbial functional responses and (c) microbial temperature adaptive responses

a) Environmental drivers of richness					
Bacteria					AIC = 133
Fixed effects	*Estimate*	*SE*	*d.f.*	*t value*	*P value*
+3°C warming	-43.2	36.5	11	-1.2	0.26
+8°C warming	-350.9	56.4	11	-6.2	<0.001 ***
Soil moisture	-216	370.3	11	-0.6	0.57
Random effect (space: plot pair)	663.3	142	11	4.67	<0.001 ***
Fungi					AIC = 86
Fixed effects	*Estimate*	*SE*	*d.f.*	*t value*	*P value*
+3°C warming	-37.8	10.4	6	-3.6	0.0105 *
+8°C warming	-66.2	23	9	-2.9	0.0187 *
Soil moisture	75.9	146.1	9	0.5	0.6163
Random effect (space: plot pair)	122.6	55.5	9	2.2	0.0559
b) Microbial functional correlates of richness					
Bacteria					AIC = 171
Fixed effects	*Estimate*	*SE*	*d.f.*	*t value*	*P value*
CO_2 efflux	-10.3	2.1	12	-4.9	<0.001 ***
micC	-0.6	0.1	12	-5	<0.001 ***
Random effect (space: plot pair)	714	42	12	17	<0.001 ***
Fungi					AIC = 112
Fixed effects	*Estimate*	*SE*	*d.f.*	*t value*	*P value*
CO_2 efflux	-1.8	0.3	7	-5.7	<0.001 ***
micC	-0.2	0.02	7	-8.9	<0.001 ***
Random effect (space: plot pair)	178	7.6	10	23	<0.001 ***
c) Microbial temperature adaptation correlates of richness					
Bacteria					AIC = 22
Fixed effects	*Estimate*	*SE*	*d.f.*	*t value*	*P value*
CUE_{cn}	2.5	0.91	8	6	0.55
T_{min} of growth	-0.2	0.08	12	-2.2	0.05 *
Random effect (space: plot pair)	5.5	0.9	8	6	<0.001 ***
Fungi					AIC = 5
Fixed effects	*Estimate*	*SE*	*d.f.*	*t value*	*P value*
CUE_{cp}	1.1	1.8	8	5.8	0.55
BG_{Q10}	2.3	1.2	8	1.9	0.09
XY_{Q10}	-7.6	2.1	8	-3.6	<0.01**
T_{min} of growth	-0.1	0.05	8	-2.3	<0.05 *
Random effect (space: plot pair)	10.1	1.7	8	5.8	<0.001 ***

Extended Data Table 2 | The relationship between (a) bacterial and (b) fungal beta-diversity and edaphic environment (i), soil process rates (ii) and microbial temperature adaptive responses (iii) following 2 years of soil warming by +3 °C to +8 °C

a) Bacteria		envfit		bioenv	
Metadata set	**parameter**	**r^2**	**P-value**	**r^2**	**P-value**
i. Edaphic properties	AST	0.829	0.001	1	0.001
	H_2O	0.519	0.006		
	DOC	0.446	0.037		
ii. Microbial functional response	AG_{ase}	0.444	0.026	0.559	0.001
	BG_{ase}	0.56	0.007		
	S_{ase}	0.737	0.002	0.614	0.001
	XY_{ase}	0.519	0.009	0.456	0.002
	PX_{ase}	0.764	0.001	0.612	0.001
	CO_2	0.504	0.013		
	enzNP	0.624	0.004	0.462	0.006
iii. Temperature adaptive response	S_{Q10}	0.496	0.015	0.439	0.001
	LP_{Q10}	0.413	0.041	0.377	0.005
	T_{min} for growth	0.446	0.03	0.404	0.005
	CUE_{cp}			0.325	0.013
	P_{Q10}			0.518	0.001
b) Fungi		**envfit**		**bioenv**	
Metadata set	**parameter**	**r^2**	**P-value**	**r^2**	**P-value**
i. Edaphic properties	AST	0.485	0.037	1	0.001
	DOC	0.535	0.028		
ii. Microbial functional response (process rates)	micP	0.692	0.002		
	micCP	0.583	0.016		
	AG_{ase}	0.506	0.037		
	PX_{ase}	0.5	0.035	0.685	0.001
	enzNP	0.547	0.014	0.553	0.001
	XY_{ase}			0.505	0.002
iii. Temperature adaptive response	XY_{Q10}	0.617	0.01	0.726	0.001
	CUE_{cp}	0.479	0.035		
	T_{min} for growth	0.475	0.028	0.616	0.001

Extended Data Table 3 | The influence of soil abiotic environment on soil CO_2 efflux (a), and the effect of in situ warming levels (by +3 °C and +8 °C) on soil CO_2 efflux (b) and soil moisture (c)

a) Abiotic effects on soil CO_2 efflux				
	Parameter	SE	DF	P-value
Fixed effects				
Temperature	2.238	0.134	95.168	<2e-16 ***
Moisture	-3.659	9.193	96.702	0.691
Random effects				
Intercept (time)	-58.03	5.545	96.728	<2e-16 ***
b) Effect of warming levels on soil CO_2 efflux				
	Parameter	SE	DF	P-value
Fixed effects				
Warming (+3°C)	3.692	1.271	326	0.00392 **
Warming (+8°C)	11.249	11.249	326	6.36e-16 ***
Random effects				
Intercept (time)	4.736	0.899	326	2.47e-07 ***
c) Effect of warming levels on soil moisture				
	Parameter	SE	DF	P-value
Fixed effects				
Warming (+3°C)	-0.074	0.027	78.264	0.00799 **
Warming (+8°C)	-0.12	0.025	17.686	0.00015 ***
Random effects				
Intercept (time)	0.386	0.023	18.364	1.22e-12 ***

nature portfolio

Corresponding author(s): Andrew Nottingham

Last updated by author(s): Jun 22, 2022

Reporting Summary

Nature Portfolio wishes to improve the reproducibility of the work that we publish. This form provides structure for consistency and transparency in reporting. For further information on Nature Portfolio policies, see our Editorial Policies and the Editorial Policy Checklist.

Statistics

For all statistical analyses, confirm that the following items are present in the figure legend, table legend, main text, or Methods section.

n/a	Confirmed
☐	☒ The exact sample size (*n*) for each experimental group/condition, given as a discrete number and unit of measurement
☐	☒ A statement on whether measurements were taken from distinct samples or whether the same sample was measured repeatedly
☐	☒ The statistical test(s) used AND whether they are one- or two-sided *Only common tests should be described solely by name; describe more complex techniques in the Methods section.*
☐	☒ A description of all covariates tested
☐	☒ A description of any assumptions or corrections, such as tests of normality and adjustment for multiple comparisons
☐	☒ A full description of the statistical parameters including central tendency (e.g. means) or other basic estimates (e.g. regression coefficient) AND variation (e.g. standard deviation) or associated estimates of uncertainty (e.g. confidence intervals)
☐	☒ For null hypothesis testing, the test statistic (e.g. *F*, *t*, *r*) with confidence intervals, effect sizes, degrees of freedom and *P* value noted *Give P values as exact values whenever suitable.*
☒	☐ For Bayesian analysis, information on the choice of priors and Markov chain Monte Carlo settings
☒	☐ For hierarchical and complex designs, identification of the appropriate level for tests and full reporting of outcomes
☒	☐ Estimates of effect sizes (e.g. Cohen's *d*, Pearson's *r*), indicating how they were calculated

Our web collection on statistics for biologists contains articles on many of the points above.

Software and code

Policy information about availability of computer code

Data collection: NA

Data analysis:

Software and code used for statistical analyses and microbial community analyses (software, packages) :
R Core Team (2021). R: A language and environment for statistical computing. R Foundation for Statistical Computing, Vienna, Austria. URL http://www.R-project.org/
Vegan: Community Ecology Package (R Package Version 2 (0), 2012).
labdsv: Ordination and multivariate analysis for ecology (R package, 2017)
microbiomeMarker: microbiome biomarker analysis (2020).
hilldiv: Alberdi, A. & Gilbert, M. T. P. hilldiv: an R package for the integral analysis of diversity based on Hill numbers. bioRxiv, 545665, doi:10.1101/545665 (2019).
UniFrac:: Lozupone, C., Lladser, M. E., Knights, D., Stombaugh, J. & Knight, R. UniFrac: an effective distance metric for microbial community comparison. Isme J 5, 169-172, doi:10.1038/ismej.2010.133 (2011).
PERFect:: Smirnova, E., Huzurbazar, S. & Jafari, F. PERFect: PERmutation Filtering test for microbiome data. Biostatistics 20, 615-631, doi:10.1093/biostatistics/kxy020 (2019).
PIME: Roesch, L. F. W. et al. PIME: A package for discovery of novel differences among microbial communities. Molecular Ecology Resources 20, 415–428 (2020). doi:10.1111/1755-0998.13116
anvi'o: Eren, A Murat et al. Anvi'o: an advanced analysis and visualization platform for 'omics data. PeerJ 3 e1319 (2015). doi:10.7717/peerj.1319
phyloseq: McMurdie, P. J. & Holmes, S. Phyloseq: An r package for reproducible interactive analysis and graphics of microbiome census data. PLoS One 8, e61217 (2013). doi:10.1371/journal.pone.0061217
DADA2: Callahan, B. J. et al. DADA2: High-resolution sample inference from illumina amplicon data. Nature Methods 13, 581 (2016).

doi:10.1038/nmeth.3869
Cutadapt: Martin, M. Cutadapt removes adapter sequences from high-throughput sequencing reads. EMBnet. jour- nal 17, 10–12 (2011). doi:10.14806/ej.17.1.200

All code, reproducible workflows, and further information on data availability can be found on the project website at https://sweltr.github.io/high-temp/. The code embedded in the website is available on GitHub [https://github.com/sweltr/high-temp/] in R Markdown format. The version of code used in this study is archived under SWELTR Workflows v1.0 [https://github.com/sweltr/high-temp], DOI identifier, https://zenodo.org/badge/latestdoi/368915237

For manuscripts utilizing custom algorithms or software that are central to the research but not yet described in published literature, software must be made available to editors and reviewers. We strongly encourage code deposition in a community repository (e.g. GitHub). See the Nature Portfolio guidelines for submitting code & software for further information.

Data

Policy information about availability of data

All manuscripts must include a data availability statement. This statement should provide the following information, where applicable:

- Accession codes, unique identifiers, or web links for publicly available datasets
- A description of any restrictions on data availability
- For clinical datasets or third party data, please ensure that the statement adheres to our policy

Trimmed (primers removed) sequence data generated in this study are deposited in the European Nucleotide Archive (ENA) under Project Accession number PRJEB45074 (ERP129199), sample accession numbers ERS6485270–ERS6485284 (16S rRNA) and sample accession numbers ERS6485285– ERS6485299 (ITS). Raw fastq files can be accessed through the Smithsonian figshare, at https://doi.org/10.25573/data.14686665 (16S rRNA) and https://doi.org/10.25573/data.14686755 (ITS). All related data and data products for individual analysis workflows are available through the Smithsonian figshare under the collection: https://doi.org/10.25573/data.c.5667571

Human research participants

Policy information about studies involving human research participants and Sex and Gender in Research.

Reporting on sex and gender	NA
Population characteristics	NA
Recruitment	NA
Ethics oversight	NA

Note that full information on the approval of the study protocol must also be provided in the manuscript.

Field-specific reporting

Please select the one below that is the best fit for your research. If you are not sure, read the appropriate sections before making your selection.

☐ Life sciences ☐ Behavioural & social sciences ☒ Ecological, evolutionary & environmental sciences

For a reference copy of the document with all sections, see nature.com/documents/nr-reporting-summary-flat.pdf

Ecological, evolutionary & environmental sciences study design

All studies must disclose on these points even when the disclosure is negative.

Study description	A soil warming experiment in lowland tropical forest in Panama. The study here consists of three treatments (control, warming by 3-degrees and warming by 8-degrees) with replication of n = 5 experimental plots.
Research sample	Research samples are soil samples collected from the experimental plots systematically distributed over a 1 ha area of forest. Therefore representative of this forest a a 1 ha scale.
Sampling strategy	Sample sizes were based on n = 5 experimental plots. The 5 paired warm and control plots were situated across a 1 ha area of forest, and therefore representative of this forest (soil type, geology, floristic composition) based on 1 ha scale. Surveys of the plot area were performed prior to establishing the warming experiment to ensure that variation in soil organic matter, nutrients and CO2 efflux rates were representative and constrained at this scale. All sampling (soil chemistry, microbiology, CO2 emission) was performed at this scale, allowing us to directly relate soil biochemical processes to soil-atmosphere gas exchange.
Data collection	The data were collected using the following methods: Soil CO2 emission using an infra red gas analyser; soil nutrients, microbial

Data collection	community, microbial growth and enzymes data by collecting soil and using laboratory methods to determine metrics (see methods for protocols). Data collection was led by A. Nottingham with specific contributions from M. Montero and J. Püspök (support for field-based measurements), E. Bååth (microbial growth data) and J. Scott, K. Broders and K. Saltonstall (sequencing data).
Timing and spatial scale	The warming experiment began in 2016. The soil samples for this study were collected from the experimental warming plots 2 years later in 2018. For this study, all samples were collected and in situ measurements made during the wet season (between June and November). Therefore all data are representative of soil process rates in the absence of moisture limitation. The warming experiment represents a 1 ha area of forest therefore the results are applicable to the soil type across this 1 ha experimental plot.
Data exclusions	No data were excluded from analyses.
Reproducibility	All methods are described in detail, allowing the experimental procedure to be reproduced and verified.
Randomization	The experiment uses a paired-plot design, to address any variability due to spatial heterogeneity. Each warmed plot is paired with a neighboring control plot. The 5 paired warm and control plots are evenly spatially distributed across a 1 ha area of forest.
Blinding	Blinding not relevant to our study because it did not involve human participants

Did the study involve field work? ☒ Yes ☐ No

Field work, collection and transport

Field conditions	The study was performed in tropical rain forest situated on Barro Colorado Island in Panama. Mean annual rainfall at the study site is 2623 mm, daytime temperatures reach a high of approximately 32°C, with night-time lows of approximately 23°C. Further information on the climate at our study site is available here: https://biogeodb.stri.si.edu/physical_monitoring/research/barrocolorado
Location	Barro Colorado Island coordinates are: 9.1521° N, 79.8465° W
Access & import/export	All fieldwork and sampling was performed in compliance with national regulations, as determined by the Panamanian National Environmental Authority and as regulated by the Smithsonian Tropical Research Institute.
Disturbance	The study caused minimal disturbance, associated with collecting small volume soil samples.

Reporting for specific materials, systems and methods

We require information from authors about some types of materials, experimental systems and methods used in many studies. Here, indicate whether each material, system or method listed is relevant to your study. If you are not sure if a list item applies to your research, read the appropriate section before selecting a response.

Materials & experimental systems

n/a	Involved in the study
☒	☐ Antibodies
☒	☐ Eukaryotic cell lines
☒	☐ Palaeontology and archaeology
☒	☐ Animals and other organisms
☒	☐ Clinical data
☒	☐ Dual use research of concern

Methods

n/a	Involved in the study
☒	☐ ChIP-seq
☒	☐ Flow cytometry
☒	☐ MRI-based neuroimaging